AGU ADVANCING EARTH AND SPACE SCIENCE

Reviews of Geophysics

REVIEW ARTICLE
10.1029/2021RG000768

Key Points:

- We critically review the potential role(s) of quartz cementation as a mechanism of fault "healing" on seismic cycle timescales
- Our current understanding of silica kinetics cannot explain cementation of mesoscale fault-fracture networks within interseismic periods
- Thin principal slip zones may be cemented interseismically but a complete understanding of fault-related quartz growth requires further work

Supporting Information:

Supporting Information may be found in the online version of this article.

Correspondence to:

R. T. Williams,
rtwilliams@wisc.edu

Citation:

Williams, R. T., & Fagereng, Å. (2022). The role of quartz cementation in the seismic cycle: A critical review. *Reviews of Geophysics*, *60*, e2021RG000768. https://doi.org/10.1029/2021RG000768

Received 3 NOV 2021
Accepted 4 FEB 2022

Author Contributions:

Conceptualization: Randolph T. Williams, Åke Fagereng
Formal analysis: Randolph T. Williams, Åke Fagereng
Investigation: Randolph T. Williams, Åke Fagereng
Methodology: Randolph T. Williams
Software: Randolph T. Williams
Supervision: Randolph T. Williams, Åke Fagereng
Validation: Randolph T. Williams, Åke Fagereng
Visualization: Randolph T. Williams, Åke Fagereng
Writing – original draft: Randolph T. Williams, Åke Fagereng
Writing – review & editing: Randolph T. Williams, Åke Fagereng

The Role of Quartz Cementation in the Seismic Cycle: A Critical Review

Randolph T. Williams[1] and Åke Fagereng[2]

[1]Department of Geoscience, University of Wisconsin–Madison, Madison, WI, USA, [2]School of Earth and Environmental Sciences, Cardiff University, Cardiff, UK

Abstract Because quartz veins are common in fault zones exhumed from earthquake nucleation temperatures (150°C–350°C), quartz cementation may be an important mechanism of strength recovery between earthquakes. This interpretation requires that cementation occurs within a single interseismic period. We review slip-related processes that have been argued to allow rapid quartz precipitation in faults, including: advection of silica-saturated fluids, coseismic pore-fluid pressure drops, frictional heating, dissolution-precipitation creep, precipitation of amorphous phases, and variations in fluid and mineral-surface chemistry. We assess the rate and magnitude of quartz growth that may result from each of the examined mechanisms. We find limitations to the kinetics and mass balance of silica precipitation that emphasize two end-member regimes. First, the mechanisms we explore, given current kinetic constraints, cannot explain mesoscale fault-fracture vein networks developing, even incrementally, on interseismic timescales. On the other hand, some mechanisms appear capable, isolated or in combination, of cementing micrometer-to-millimeter thick principal slip surfaces in days to years. This does not explain extensive vein networks in fault damage zones, but allows the involvement of quartz cements in fault healing. These end-members lead us to hypothesize that high flux scenarios, although more important for voluminous hydrothermal mineralization, may be of subsidiary importance to local, diffusive mass transport in low fluid-flux faults when discussing the mechanical implications of quartz cements. A renewed emphasis on the controls on quartz cementation rates in fault zones will, however, be integral to developing a more complete understanding of strength recovery following earthquake rupture.

Plain Language Summary The strength of faults varies in time throughout the earthquake cycle. We know from laboratory experiments that fault strength decreases dramatically and instantaneously during earthquakes. Some, much, or all of that strength loss is recovered between earthquakes. This process, often referred to as fault "healing," is thought to influence the timing, location, and energy of future earthquakes. The speed and mechanism of the healing process are not well known. In many fault rocks from depths of earthquake nucleation (>10 km), seen in geological exposures, slip-related fractures and cracks are sealed with quartz cements that formed from fluids residing within, or flowing through, the fault zone. This observation has led to the common inference that quartz cementation exerts a major control on fault healing. This interpretation requires that sufficient quartz grows between successive earthquakes. We review and explore a variety of processes that have been argued to facilitate such rapid cementation. Ultimately, we find that it is difficult for quartz to grow fast enough to heal faults on the timescale of the earthquake cycle in many circumstances. Therefore, we call for more work on understanding whether quartz growth or alternative mechanisms can explain healing between earthquakes.

1. Introduction

Faults recover some, all, or more of their pre-failure strength between slip events. This recovery, often referred to as fault "healing", is an integral component of the seismic cycle and thought to govern earthquake repeat times (e.g., Marone, 1995; Sibson, 1992, 1995; van den Ende & Niemeijer, 2018), stress drops (e.g., Karner & Marone, 2000; Marone, 1995), rupture propagation (e.g., Beeler & Tullis, 1996; Williams, Mozley, et al., 2019), and seismic energy release (e.g., Kanamori & Allen, 1986; McLaskey et al., 2012). Lack of healing may also control the propensity for stable, aseismic fault creep (e.g., Carpenter et al., 2011). Experimentally, healing has been described as an effect of the time-dependency of the coefficient of friction (Dieterich, 1972; Marone, 1998), and as an effect of time-dependent cohesion (Muhuri et al., 2003; Tenthorey & Cox, 2006; Van den Ende & Niemeijer, 2019). Healing thereby occurs through a combination of mechanical and chemical processes, including

grain rotation and/or bonding, recrystallization, and the serial processes of dissolution, diffusion, and precipitation, taken together sometimes referred to as pressure solution (Rutter & Elliott, 1976). As this term technically refers to the dissolution of material at a stressed grain boundary (Durney, 1972), we use the more explicit phrase "dissolution-precipitation creep" to differentiate the dissolution process from the combined processes resulting in strain. Although increases in real contact area over time can lead to recovery of frictional resistance in dry conditions (Dieterich, 1972), it is generally accepted that fluid flow through damaged rocks enhances the healing processes listed above (Olsen et al., 1998; Renard et al., 2000; Tenthorey et al., 2003), and in experiments and models, fluid-driven healing along fault planes can modulate the earthquake cycle (Hooker & Fisher, 2021; Van den Ende & Niemeijer, 2019).

In the context of fluid-enhanced healing, the cementation of fractures or cracks by deposition of minerals precipitating from a fluid acts to increase cohesive strength (e.g., Karner & Marone, 2000; Muhuri et al., 2003; Sibson, 1992; Tenthorey & Cox, 2006; Tenthorey et al., 2003). The common observation of mineral cements in exhumed faults, which are commonly found in abundances that far exceed those in the surrounding protolith (e.g., Breeding & Ague, 2002; Cox, 1995; Eichhubl et al., 2009; Faber et al., 2014; Micklethwaite & Cox, 2004; Williams et al., 2016; Williams, Goodwin, et al., 2015), suggest that cementation may play a key role in fault healing. Quartz cements, although common throughout the continental crust, are particularly prevalent near the base of the seismogenic zone (Bestmann et al., 2016; Boullier & Robert, 1992; Fagereng et al., 2011, 2018; Melosh et al., 2014; Ujiie et al., 2018) where the kinetics of silica dissolution, transport, and precipitation are relatively rapid (Lander & Laubach, 2015; Lander et al., 2008; Rimstidt & Barnes, 1980). In faults exhumed from these temperatures and depths (i.e., ~300°C–350°C and 10–15 km in continental crust, but deeper in subduction zones; Sibson, 1982), quartz is frequently observed cementing gouge/cataclasite along fault interfaces and/or sealing larger dilatant fractures in the surrounding damage zones (e.g., veins and breccias; Figures 1–3). In particular, veins and cements have been reported to fill and affect the strength of the fault core in several exhumed examples (e.g., Callahan et al., 2020; Cox, 1995; Nguyen et al., 1998), although the potential spatial extent of such cementation is unclear, largely from the inherent scale limitations of outcrop studies. Thus, quartz cementation likely provides a fundamental mechanism for reducing damage accrued during fault slip, and may influence the strength, permeability, and viscosity of fault zones at the depths where most large ($Mw \geq 6$) earthquakes nucleate (Jiang & Lapusta, 2017; Sibson, 1982). Understanding the potential role(s) of quartz cementation in this process, however, requires balancing the rates of quartz precipitation and strain accumulation over the full range of spatial and temporal scales relevant to the seismic cycle.

Two criteria must be met in order for fault healing by quartz cementation to have an impact on the seismic cycle. First, for strength to recover, the volume of cement precipitated must be sufficient to at least partially close cracks/fractures, either along the fault interface or in the surrounding damage zones. Second, the rate at which these cements are precipitated must be fast enough for the strength and permeability of faults to be affected on time scales shorter than their interseismic period (a few 100 years or less in active, plate-boundary fault systems; Williams, Davis, & Goodwin, 2019). The process and efficiency of cementation, however, likely depends in some part on hydraulic regime (Cox, 2010). A diffusive end-member likely occurs, for example, in systems where either rock permeability and/or the prevailing hydraulic gradient prevents significant fluid flux, and cementation procedes predominantly by local dissolution-precipitation creep (e.g., Cox, 2010; Laubach et al., 2014, 2019). On the other hand, an advective end-member may occur where faults are episodically connected to highly overpressured reservoirs when fault slip results in increased permeability, leading to transient high fluid flux along the fault (Cox, 1995; Sibson, 1992, 1995; Sibson et al., 1988). Intermediate cases are also possible, and spatial variabilities in hydraulic regime may occur because of local differences in deformation mechanisms and permeability production within individual fault zones (e.g., Caine et al., 1996). In this way, the concept of healing may be considered relative to the two primary elements of fault zone architecture: discrete fault surfaces and their surrounding damage zones. Deformation along individual fault surfaces largely takes the form of mechanical wear and grain comminution during slip. The collective result of these processes is the production of very low porosity/permeability cataclasite or fault gouge, where cementation is likely governed predominately by diffusion in a low-flux environment. Exceptions may occur at geometrical complexities, such as fault bends and step-overs, where fault permeability could be locally elevated (Peacock et al., 2017; Weatherley & Henley, 2013). Cementation of materials along the fault interface has direct implications for the stability and strength of faults and the propensity for additional slip. Deformation in the surrounding damage zones, in contrast, is arguably more variable across individual fault systems, although dilatant deformation in the form of micro-to-meter-scale fracturing

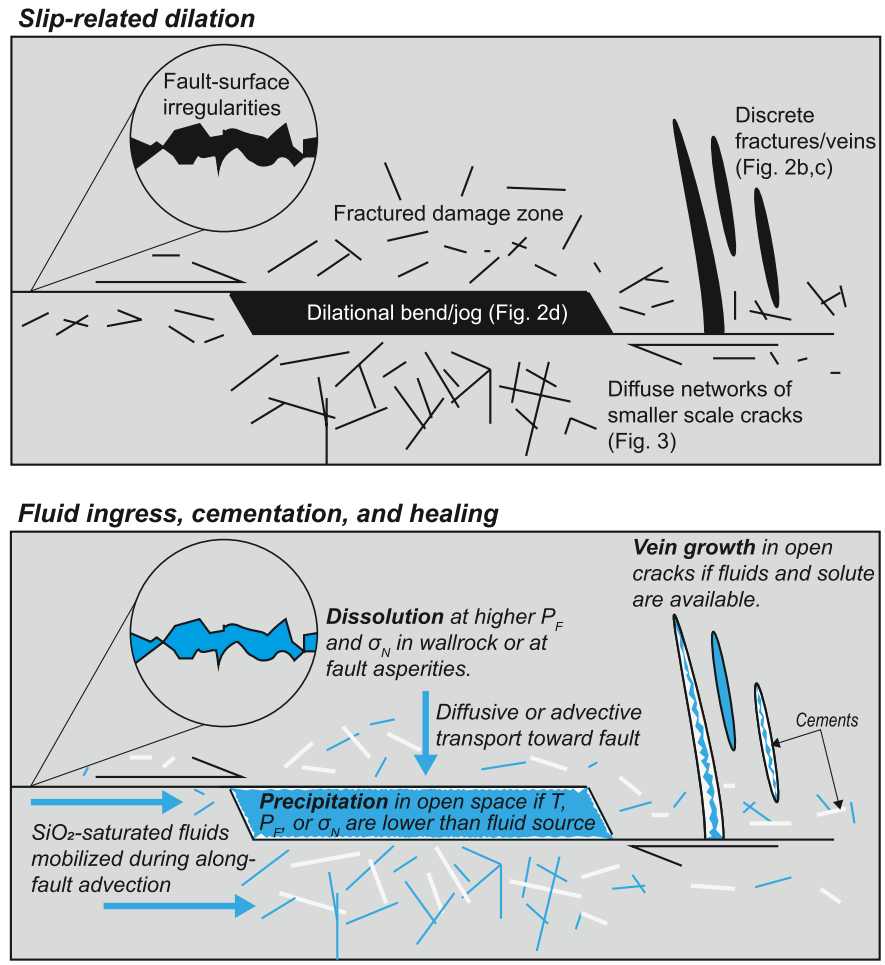

Figure 1. Schematic diagram illustrating slip-related dilation and mechanisms of fluid ingress, cementation, and sealing. Simply stated, quartz cementation in fault zones requires a change in the relative supersaturation of silica in migrating fluids. The slip-related mechanisms of varying silica supersaturation, and their impact on fault healing and the seismic cycle, are the primary focus of this paper.

and brecciation is common (e.g., Caine et al., 1996; Cox, 1995; Faleiros et al., 2014; Laubach et al., 2014; Melosh et al., 2014; Nguyen et al., 1998; Woodcock et al., 2007). Damage zone cementation may therefore also be controlled by diffusion in low-flux environments, or alternatively by advection in high-flux environments given the highly permeable nature of fractured/brecciated rock relative to its undeformed state. Cementation of fracture networks in fault damage zones is unlikely to directly impact fault strength, but is likely to have ancillary impacts on overall fault-zone permeability (including the potential to localize pore-fluid overpressures consequent to fault weakening) and mechanical compliance and/or elasticity (with implications for seismic wave propagation).

In this paper, we explore the variety of slip-related mechanisms that have been argued to allow quartz cementation and associated healing in faults over interseismic time scales. We consider quartz cementation to close cracks/fractures (opening-mode or hybrid), including both aggregate cementation of microfractures or pore space in breccias, cataclasites, or gouges along fault surfaces in addition to sealing of more discrete, mesoscale structures in fault damage zones (Figures 2 and 3). We hereafter use the term "fracture cementation" and "sealing" to encompass the filling of fractures with quartz cement and any associated mechanical or hydrological response. Our goal is to leverage the existing literature to assess the rate, duration, and magnitude of cementation that may result from each driver of quartz precipitation, and determine their potential to contribute to fault healing over typical interseismic time scales in the seismogenic crust. In particular, we focus on processes occurring near the base of the seismogenic crust (i.e., temperatures of 300°C–350°C; 10–15 km depth in continental crust but deeper in subduction zones) where most large earthquakes nucleate and where the potential for fault healing facilitated

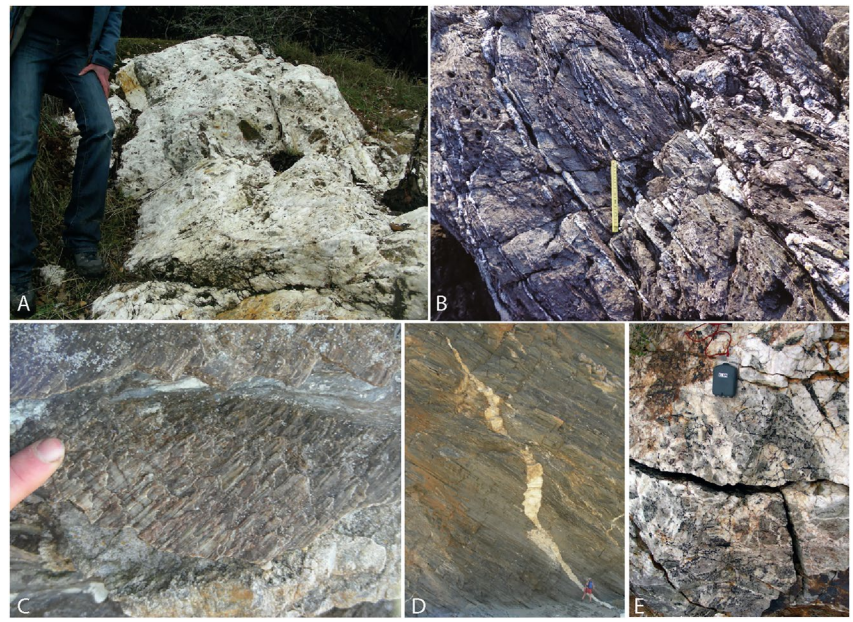

Figure 2. Outcrop images of quartz cements in faults. (a) Meter-scale quartz vein associated with the Motherlode gold deposits of California, USA. Person for scale. (b) Discrete quartz veins cutting metapelites in the Makimine Mélange, Kyushu, Japan. Pencil scale. (c) Quartz slickenfibers filling centimeter-scale dilational jogs in Chrystalls Beach, New Zealand. Finger for scale. (d) Vein filling a fault-localized fracture in the Kuiseb Schist, Kuiseb Canyon, Namibia. The person in the bottom right of the image is approximately 1.5 m tall. (e) Vein partially filled with euhedral quartz crystals, Cape Fold Belt, South Africa. Compass for scale.

by quartz cementation is highest. The key conclusion is that such healing by cementation, although commonly invoked, is most easily explained in very low porosity fracture systems along fault interfaces, while cementation of more extensive vein systems in fault zones requires conditions that are rarely achieved if currently known empirical relations are correct.

1.1. Quartz Growth Rates in Fault Zones at Earthquake Nucleation Depths: Current Understanding of Kinetic Constraints

The rates of silica dissolution, diffusion, and precipitation increase exponentially with temperature (e.g., Fournier & Potter, 1982b; Rimstidt & Barnes, 1980). The greatest potential for quartz cementation to significantly affect fault healing is therefore near the base of the seismogenic crust (i.e., the warmest part of the crust deforming primarily by brittle deformation). In the continents, this depth is resolvable in catalogs of earthquake hypocenters (Sibson, 1982) and likely coincides with the onset of efficient ductile deformation in quartz at ~300°C–350°C. Unfortunately, very little is known about the rates of quartz precipitation in fault zones at these depths from direct analysis of the rock record. Rather, the overwhelming majority of our knowledge of silica kinetics in fault zones is inferred from laboratory experiments (e.g., Brantley et al., 1990; Rimstidt & Barnes, 1980; Tenthorey & Cox, 2006; Tenthorey et al., 2003; Williams, Farver, et al., 2015) or theoretical models (e.g., Renard et al., 2000), although such constraints have been applied to explain direct geological observations (Faber et al., 2014; Fisher et al., 2019; Hooker & Fisher, 2021; Saishu et al., 2017; Ujiie et al., 2018).

Empirical constraints on the potential rates of quartz cementation (i.e., those derived from analysis of the rock record or laboratory-synthesis experiments) are focused almost exclusively on diffusion-controlled precipitation in low-flux environments. A large body of research has attempted to place constraints on the rates of quartz cementation in fractures in sedimentary reservoir rocks under near-equilibrium, diagenetic conditions in particular (i.e., <~200°C; see review by Laubach et al., 2019). For example, fluid-inclusion microthermometry of crack-seal quartz veins in sandstone reservoirs has been used to estimate average rates of fracture opening and vein formation of ~25 μm per million years at ~100°C–175°C (Becker et al., 2010; Fall et al., 2015; Hooker et al., 2015). If this rate is taken as synonymous with the rates of quartz precipitation in each vein (given the multiply-refractured,

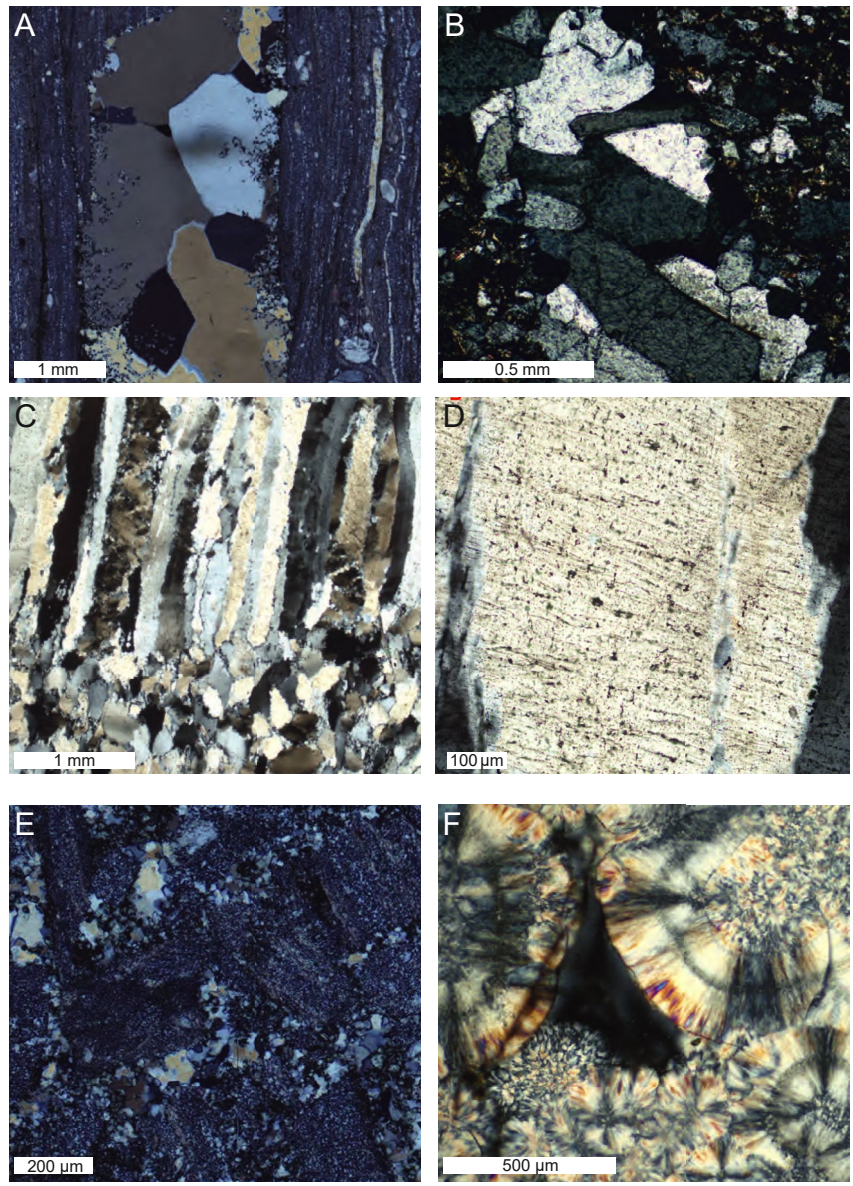

Figure 3. (a) Blocky quartz recording cementation of a large (~2 mm aperture) dilatant shear fracture. (b) Blocky quartz recording cementation of a smaller (~500 µm) opening-mode fracture. (c) Fibrous or "stretched" quartz crystals recording repeated (re)opening and (re)sealing of small increments. (d) Sub-parallel fluid inclusion planes delineating "crack-seal" increments in panel (c). Opening increments are generally approximated as the average distance between fluid inclusion planes (here ~10–30 µm). (e) Mosaic quartz cements filling pore space in a dilational breccia in mylonite. (f) "Flamboyant" spheroids of epithermal quartz interpreted to record recrystallization from a metastable precursor phase.

crack-seal nature of the veins the rate is more accurately considered a minimum estimate of precipitation rate), then it is generally compatible with that predicted by kinetic-rate equations developed by Lander et al. (2008), who employ a standard Arrhenius formulation with activation energy and pre-exponential factor estimated from observed accumulations of natural quartz cements in reservoirs rocks with known time-temperature histories. The Lander et al. (2008) model was subsequently redeployed by Lander and Laubach (2015) to define structural-kinetic models of quartz cementation in fractures during repeated episodes of reactivation. Both of these models predict maximum quartz precipitation rates on the order of ~1 mm per million years (10^{-3} µm/year) at 350°C (i.e., the base of the seismogenic crust; Figure 4). These rates imply sub-µm cement accumulations over the 100-year interseismic timescales typical of active, plate-boundary faults. It is conceivable that such modest accumulations of cement may be capable of altering the mechanical properties of very low porosity cataclasites

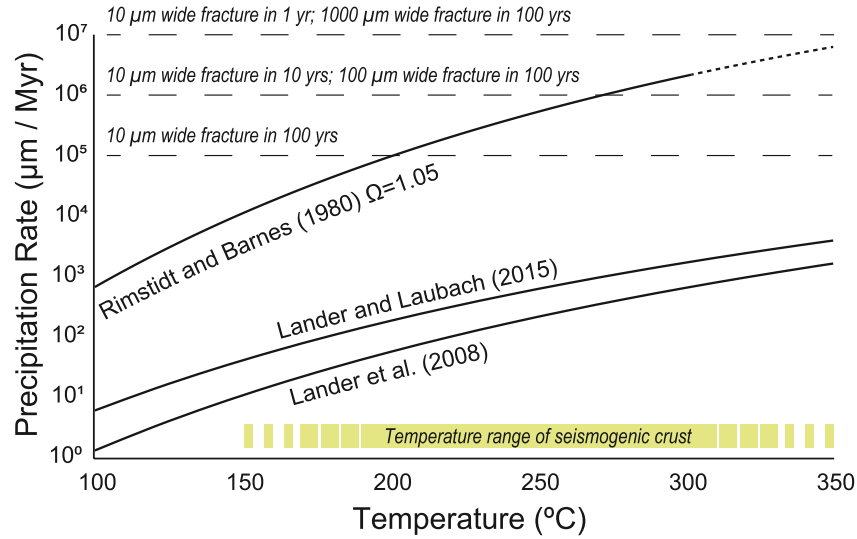

Figure 4. Plot illustrating quartz precipitation rates as a function of temperature from kinetic rate models (solid lines). Rates predicted by Lander et al. (2008) and Lander and Laubach (2015) represent estimates for non-euhedral, c-axis-parallel (i.e., maximum) growth. Rates predicted by Rimstidt and Barnes (1980) incorporate effects associated with silica supersaturation (in this case $\Omega = 1.05$), but are non-specific with respect to crystallographic orientation and euhedralism of the host grains (explained below). Estimates from Rimstidt and Barnes (1980) are extrapolated from temperatures of 300°C to respect the constraints of the original experimental calibration. Dashed horizontal lines indicate precipitation rates required to seal fractures of various widths over time scales relevant to the seismic cycle (i.e., a few 100 years or less).

localized along discrete fault surfaces over the 100-year time scales typical of an interseismic period (e.g., Renard et al., 2000; Tenthorey & Cox, 2006; Yasuhara et al., 2005), but they are certainly not capable of sealing larger fractures (whose opening increments may range from 10s of μm to cm in scale) commonly observed in fault zones exhumed from seismogenic depths (Figure 4). Thus, as applied to dilational deformation in fault damage zones, the diffusion-controlled models of Lander et al. (2008) and Lander and Laubach (2015) stand in contrast to an abundance of outcrop and microstructural evidence in exhumed fault rocks, which appear to record a seismic cycle characterized by intermittent but numerous episodes of quartz cementation and fracture sealing between discrete slip events (e.g., Boullier & Robert, 1992; Cox, 1995; Fagereng et al., 2011, 2018; Renard et al., 2005; Sibson et al., 1988; Ujiie et al., 2018; Figures 2 and 3). The precipitation rates estimated by Lander et al. (2008) and Lander and Laubach (2015), however, do not include a term for the effect of silica supersaturation (i.e., the ratio of the concentration of silica in pore fluid to that at equilibrium):

$$\Omega = CSiO_2/CSiO_{2-eq} \quad (1)$$

Precipitation in the Lander et al. (2008) and Lander and Laubach (2015) models is instead assumed to occur from fluids that are near equilibrium with respect to silica concentration (i.e., $\Omega \sim 1$), consistent with the conditions anticipated for quartz precipitation governed principally by diffusion in a low fluid flux environment. As such, precipitation rates in the Lander et al. (2008) and Lander and Laubach (2015) models are not appreciably influenced by fluid advection or dynamic changes in pressure, temperature or other variables, but rather are controlled entirely by ambient temperature and the crystallographic nature of the quartz growth surface (i.e., fast *c*-axis vs. slow *a*-axis growth, fast growth on anhedral surfaces vs. slow growth on euhedral terminations; see Lander et al. (2008) for a complete discussion). The assumption of near-equilibrium conditions also implies nucleation barriers inherent in quartz precipitation that dictate growth should occur exclusively on quartz grains within a rock mass. Lander and Laubach (2015) showed that the collective effect of these factors results in a potential for fracture sealing that is dependent only on temperature and the morphology and orientation of quartz grains in the fracture walls relative to the rate of fracture opening. This model has proven effective in reproducing the characteristics of cemented fractures inferred to have formed under near-equilibrium silica concentrations below ~250°C (which are commonly discontinuously cemented across their extent; e.g., Becker et al., 2010; Fall et al., 2015; Hooker et al., 2015; Laubach et al., 2014; Wang et al., 2019). It is important to note, however, that

(Lander & Laubach, 2015) specifically recognized that the assumption of near-equilibrium silica concentrations may be violated at depths and temperatures beyond those typical of reservoir diagenesis.

In the vicinity of active, seismogenic faults near the base of the seismogenic crust, for example, fluid flux can vary substantially with time (e.g., Braun et al., 2003; Husen & Kissling, 2001), and fluids may experience rapid changes in pressure, temperature, and other variables that directly or indirectly affect solubility and thus lead to supersaturation (Cox, 1995; Saishu et al., 2017; Sibson, 1992; Ujiie et al., 2018). In fact, the microstructures of quartz cements in many fault systems exhumed from these depths reveal a critical difference in the mechanisms of cementation when compared to reservoir diagenetic examples that are well explained by the Lander and Laubach (2015) model: inferred fracture opening increments are typically entirely sealed with quartz cement (although exceptions may occur; e.g., Ague, 1995; Fisher & Byrne, 1990), regardless of protolith type or the mineralogy/orientation/size of individual grains in the fracture wall (Figure 3; see examples in Cox, 1987, 1995; Fagereng et al., 2011; Melosh et al., 2014; Saishu et al., 2017; Ujiie et al., 2018). These microstructures may imply that the strict nucleation barriers inherent under near-equilibrium conditions (and recorded in the discontinuously quartz cemented fractures of Becker et al., 2010; Fall et al., 2015; Hooker et al., 2015; Lander & Laubach, 2015; Laubach et al., 2014; Wang et al., 2019; in addition to others) are not necessarily operative in active faults experiencing quartz cementation near the base of the seismogenic crust. The lack of such strict nucleation barriers during quartz precipitation implies increased silica supersaturation during cementation, perhaps resulting from dynamic variations in equilibrium silica solubility throughout the seismic cycle. Indeed, it would seem that supersaturation is required to explain the large disparity in quartz cementation rate between what is predicted by the models of Lander et al. (2008) and Lander and Laubach (2015) and what is required to seal the 10s of μm to cm fracture opening increments observed in some exhumed faults over interseismic timescales (i.e., a few 100 years or less; Figure 4).

1.1.1. A Tentative Resolution for Dilatant Faults and Fractures

If laboratory constraints on silica kinetics are taken to be broadly accurate in determining the primary controls on quartz precipitation rate, then the potential for fault healing through quartz cementation is largely dependent on temperature, silica supersaturation, and mass flux of silica during and after fault slip. Assuming the main fluid phase available to transport dissolved silica is H_2O, silica solubility depends on the temperature, pressure, pH, and salinity of aqueous fluids. Of these, the effects of changing temperature and pressure are well constrained by experimental and theoretical studies, and these parameters likely experience substantial variations over the temporal and spatial scales of the earthquake cycle. Decreases in fluid temperature, for example, may occur when hot, silica-saturated fluids ascend inclined faults or fractures and cool at higher structural levels following rupture and associated increases in fault permeability. Decreases in fluid pressure may similarly occur during coseismic dilational deformation or post-seismic discharge of fluids from previously overpressured horizons—particularly if a rupture disrupts a hydrological barrier bounding an overpressured compartment (e.g., Cox & Munroe, 2016; Miller & Nur, 2000; Sibson, 1992). Both of these processes occur in advective regimes and result in local and rapid decreases in the equilibrium solubility of silica in pore fluids, resulting in corresponding increases in the degree of local supersaturation and rates of quartz precipitation (i.e., $CSiO_{2-eq}$ in Equation 1 decreases). Experimental work has shown, for example, that quartz precipitation rates at a constant temperature vary as an approximately linear function of Ω-1 (Rimstidt & Barnes, 1980) (Most previous work in mineral kinetics [including Rimstidt and Barnes (1980)] describes the departure from equilibrium concentration as (1-Ω) by convention, resulting in rates of mineral dissolution that are positive and rates of mineral precipitation that are negative. As this work is focused on rates of precipitation, we recast the term describing the departure from equilibrium concentration as (Ω-1), resulting in positive rates of precipitation.). Estimation of quartz growth rates using these laboratory derived constraints, however, yields precipitation rates several orders of magnitude larger than those provided by the naturally-parameterized models of Lander et al. (2008) and Lander and Laubach (2015). Several factors may explain the discrepancy between the two empirical models, and between the rates determined by Lander et al. (2008) and Lander and Laubach (2015) and the rates required by the rock record of fault-related veins. First, although thermodynamic theory predicts a linear relationship between precipitation (or dissolution) and $\Omega - 1$ (Lasaga, 1981; Palandri & Kharaka, 2004), experiments have shown that pronounced non-linearities in reaction rate may exist between near-equilibrium and moderately supersaturated solutions for some minerals (Burch et al., 1993; Nagy & Lasaga, 1992). Critically, quartz precipitation experiments are only conducted at

moderate-to-high supersaturations to yield quantifiable growth over laboratory time scales. As such, the effects of supersaturation on reaction rates between the near-equilibrium conditions incorporated into the pre-exponential factor of Lander et al. (2008) and the experimentally-calibrated models of Rimstidt and Barnes (1980) are entirely unknown from direct analysis, and quite possibly non-linear. Second, the kinetic-rate constants in Lander et al. (2008) and Lander and Laubach's (2015) model are derived from observation of natural quartz overgrowths in reservoir sandstones, and according to those authors inherently incorporates effects associated with "nucleation discontinuities" on the surface of detrital grains (e.g., clay or oxide coatings, organic residues, etc.). These effects are unlikely to be important, or even present, on the surface of fresh fractures in fault zones. In fact, Spruženiece et al. (2021) demonstrated that natural blocky calcite veins can only be simulated numerically if growth is faster on transgranular fractures than on intergranular surfaces. In quartz, hydrothermal experiments on fractured detrital-quartz grains in supersaturated solutions also demonstrate this effect (Williams, Farver, et al., 2015), and show that the rates of quartz precipitation on fresh fracture surfaces subjected to supersaturated conditions are more consistent with those predicted by Rimstidt and Barnes (1980) than Lander et al. (2008) and Lander and Laubach (2015).

In this paper, we use the constitutive equations of Rimstidt and Barnes (1980) to estimate the rates of quartz cementation in fault zones in a series of generalized cases to analyze the effects of isolated parameters. Although this is the most appropriate empirical model for post-seismic quartz precipitation available to us, we stress that until more direct constraints on the rates of quartz precipitation in the seismogenic crust can be obtained, the rates calculated here should be taken with caution, or perhaps even mild skepticism. In particular, we note that the experiments of Rimstidt and Barnes (1980) were conducted in a closed system, but that they specifically quantified variations in quartz precipitation as a function of temperature and changing silica supersaturation. The application of these constraints to open-system scenarios in the crust is made on the assumption that such systems provide a mechanism of increasing silica mass balance, and therefore maintaining high degrees of supersaturation throughout crystal growth.

Rimstidt and Barnes (1980) provide a general equation for predicting the rate of accumulation (r_{sfc} in m/s) of quartz on a surface (sfc) of the following form:

$$r_{sfc} = kV_{qtz}(\Omega - 1) \tag{2}$$

Where k is a temperature-dependent rate constant (s^{-1}), V_{qtz} is the molar volume of quartz (22.55 cm^3/mol), and Ω is the degree of supersaturation (unitless; Equation 1). This formulation is directly constrained for temperatures up to ~300°C (coinciding with the approximate base of the continental seismogenic crust; Sibson, 1982) and relies on several assumptions. First, crystal nucleation and growth are assumed to occur as quartz rather than amorphous silica or other metastable precursors. Second, the reaction is assumed to proceed under a constant degree of supersaturation with infinite fluid and solute availability. The validity of the first assumption will be addressed in the following section. The second implicitly assumes that fluid flux is sufficiently high to not place limits on precipitation rate, and its validity is almost certainly variable as a function of depth and lithology in the crust in addition to the mechanism invoked for generating the supersaturations required for precipitation (discussed in detail below). As such, its validity will be discussed in each of the individual sections on slip-related mechanisms leading to increased rates of quartz cementation. We recognize that the Rimstidt and Barnes (1980) formulation is non-specific with respect to variations in quartz precipitation rate that may arise as a function of the crystallographic nature or orientation of the substrate (i.e., fast *c*-axis vs. slow *a*-axis growth, fast growth on anhedral surfaces vs. slow growth on euhedral terminations; see Lander et al., 2008). Given that their formulation is based on experimental determination of aggregate precipitation rates in a granular mass of quartz grains, however, it is likely that most surfaces were anhedral and all potential crystallographic axes were on some level represented. Thus, the precipitation rates we estimate likely represent an average anhedral rate normalized across a wide range of crystallographic axes. Finally, we recognize that this approach neglects the potential for decreases in quartz precipitation associated with the development of euhedral terminations during fracture cementation, and we refer the reader to the work of Lander and Laubach (2015) for a more indepth consideration of that possibility. Here, we simply emphasize that such terminations are generally absent in crack-seal veins exhumed from near the base of the seismogenic crust, and also that the neglect of precipitation rate variations due to the onset of euhedralism implies that any quartz precipitation rates we estimate using this approach could reasonably be

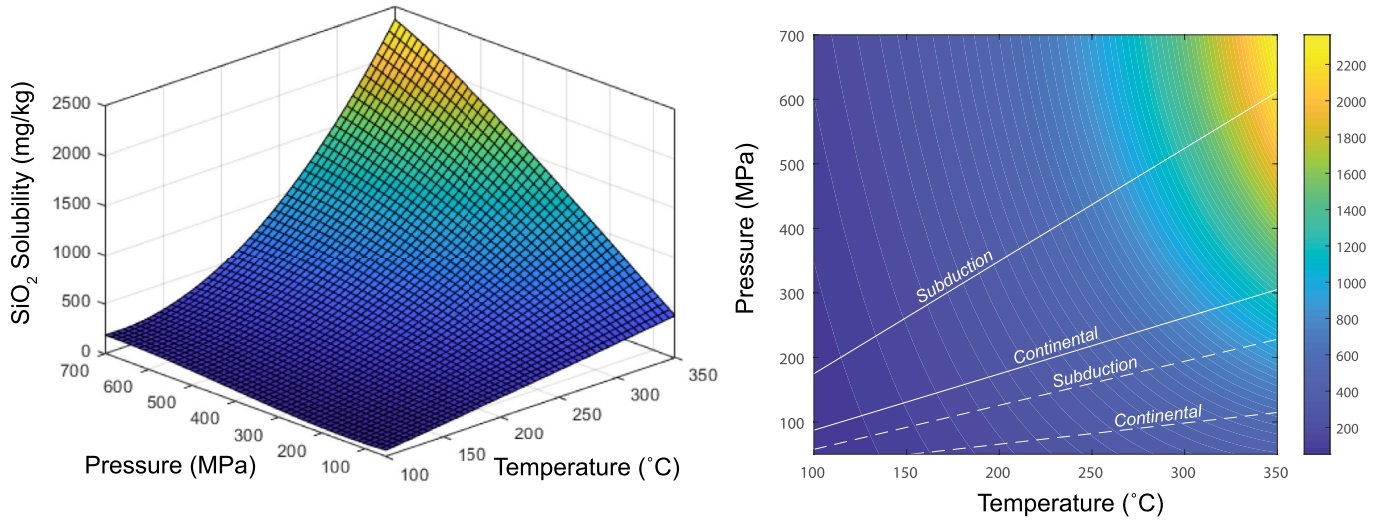

Figure 5. (Left) Surface plot showing the solubility of silica (mg SiO_2/kg water, or "parts per million") as a function of temperature and pressure in the crust. The effect of pressure is relatively limited at temperatures below ~250°C. (Right) Color-shaded contour showing silica solubility as a function of temperature and pressure. Dashed and solid lines show hydrostatic and lithostatic gradients, respectively, for linear geothermal gradients appropriate to continental crust (30°C/km) and subduction zones (15°C/km).

considered maximum values (implying that any associated fracture sealing times are minima; see below for more details).

1.1.2. Equilibrium Silica Solubility

To assess the effect of changes in the equilibrium solubility of silica on quartz precipitation rates in fault zones, the pre- and post-failure solubility of silica must first be established. Manning (1994) provides an experimentally-derived equation for estimating the solubility of silica with respect to quartz as a function of temperature and density of water. This calibration extended previous work (cf. Fournier & Potter, 1982b) with an improved experimental methodology, and was later validated by thermodynamic modeling of Dolejš and Manning (2010). The density of water, however, is not an intuitive parameter for estimating pre-failure solubility at a particular depth in the crust. As a solution, we conducted a 3D surface fit to combined temperature, pressure, and specific volume data obtained from the United States National Institute of Standards and Technology (NISTIR 5078). The resulting fit equation estimates specific volume as a function of temperature and pressure with errors less than 0.02% relative to accepted values. A more complete description of this approach, and the resulting equations, are available in Supporting Information S1. We then used this fit equation in conjunction with equations from Manning (1994) to estimate silica solubility with respect to quartz over a range of conditions representative of the seismogenic crust (e.g., Figure 5).

2. Quartz Precipitation in the Seismic Cycle

In this section, we examine processes that have been invoked to drive quartz cementation, and consider whether they allow precipitation of a sufficient amount of cement fast enough to be viable mechanisms for cementation and fracture sealing on the timescale of a typical interseismic period (i.e., a few 100 years or less). For the sake of temporal considerations, many of the discussions below consider the time required to completely cement/seal a discrete fracture of a specified aperture. No specificity is implied with respect to the location, orientation, or frequency of those fractures within an overall fault zone, nor to the possibility of partial sealing. Finally, we restrict our analyses to a temperature range of ~150°C–350°C as being generally representative of conditions within the seismogenic crust. We place a particular emphasis on processes occurring in the deepest portions of the seismogenic crust (i.e., ~300°C–350°C; 10–15 km in continental crust but deeper in subduction zones) where most large earthquake nucleate (Sibson, 1982), and thus where quartz cementation and any associated

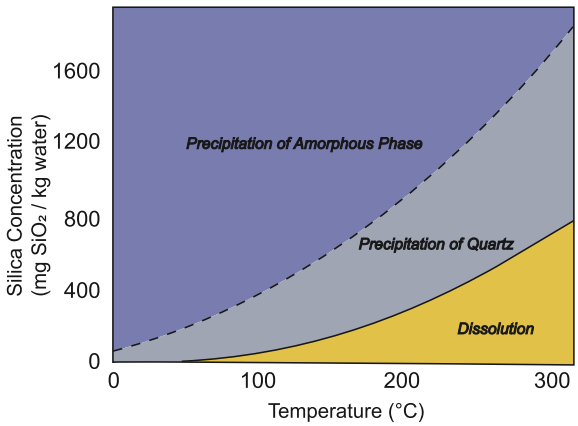

Figure 6. Equilibrium solubility of quartz (solid line) and amorphous silica (dashed line) in pure water as a function of temperature at vapor pressure. To precipitate amorphous silica, the concentration of silica in pore-fluids must exceed the equilibrium solubilities of both quartz and amorphous silica. Supersaturation with respect to quartz is therefore always achieved at lower silica saturation compared to that required for precipitation of amorphous silica. The difference in the equilibrium solubility of quartz and amorphous silica decreases with decreasing temperature, such that amorphous silica is more likely to precipitate in fractures at low temperature conditions, that is, at relatively shallow depths. Modified from Rimstidt and Cole (1983).

mechanical modification has the greatest potential to facilitate healing in the seismic cycle.

2.1. Precipitation of Amorphous Silica

Amorphous and/or metastable silica phases may precipitate at rates well in excess of those expected for quartz because of their decreased activation energies and therefore faster reaction kinetics (Rimstidt & Barnes, 1980). Recognizing this, several previous studies have proposed that initial precipitation of these phases may provide a mechanism for rapidly cementing faults during the seismic cycle. At temperatures consistent with much of the seismogenic crust, amorphous phases would likely experience subsequent recrystallization over relatively short time scales to become the more stable quartz observed in exhumed fault rocks (Bettermann & Liebau, 1975; Herrington & Wilkinson, 1993; Williams, Farver, et al., 2015; Yilmaz et al., 2016). Rock record evidence for this mechanism of cementation is therefore inferred from the presence of stable quartz with preserved flow banding, spherules/colloids, and accumulations of micro-to-nano scale anhedral quartz and/or hydrous crystalline and amorphous silica in fault veins and on slip surfaces (Figure 3f; Borhara & Onasch, 2020; Dong et al., 1995; Faber et al., 2014; Kirkpatrick et al., 2013; Moncada et al., 2012; Onasch et al., 2010; Yilmaz et al., 2016). These examples, however, are all a product of silica precipitation at relatively shallow depths in the crustal seismogenic regime (<300°C).

Precipitation of amorphous silica cannot occur unless the concentration of silica in pore fluids exceeds that of the equilibrium concentration with respect to the amorphous phase in question (Figure 6). Given that the solubility of many of these phases is up to a factor of three larger than that of quartz under the same conditions (Dove, 1994), supersaturation with respect to quartz must by definition be achieved before that with respect to other amorphous and/or metastable silica phases. The potential for precipitation of amorphous or metastable silica phases therefore depends on the rate of quartz precipitation relative to that of the rate of increases in silica saturation. Where quartz growth rates are relatively fast, precipitation forms a negative feedback reaction and competes with the mechanism(s) increasing silica concentration, likely preventing sufficient supersaturation to precipitate the amorphous or metastable phase. The precipitation of these phases is therefore most probable at shallow depths where the kinetics of quartz precipitation are relatively slow, and the difference between the equilibrium solubilities of quartz and amorphous silica is relatively small. Indeed, this is consistent with the rock record as outlined above, and in addition, hydrothermal experiments have shown that at 300°C, precipitation occurs directly as quartz even when the solution is in equilibrium with amorphous silica (Williams, Farver, et al., 2015). As such, it is likely that precipitation near the base of the seismogenic crust occurs predominately as quartz rather than a precursor, amorphous or metastable phase. This conclusion is broadly consistent with many quartz veins observed in exhumed seismogenic faults, where common syn- and antitaxial microstructures record a crystallographic control on the habit of cements (e.g., Figure 3c; Bons et al., 2012; Boullier & Robert, 1992; Cox, 1987, 1995; Fagereng et al., 2011; Ujiie et al., 2018), but does not exclude non-crystalline silica precipitation under certain special circumstances of extreme supersaturation (e.g., Herrington & Wilkinson, 1993) or that amorphous precipitation has taken place in examples where primary growth textures are masked by later recrystallization.

It is possible that sufficient supersaturation can be reached for amorphous or other metastable silica phases to precipitate directly from solution in exceptional cases, such as during rapid coseismic depressurization and fluid vaporization (e.g., Amagai et al., 2019; Weatherley & Henley, 2013). The extent to which these processes are likely to occur in the seismogenic crust was discussed in part by Williams (2019), and is considered further below.

2.2. Rates of Quartz Precipitation During Fluid Advection

Variations in temperature and pressure during fluid advection influence both the reaction kinetics and equilibrium solubility of silica. Where pore-fluid pressure gradients exceed hydrostatic values, fluids may ascend through the crust along vertical and inclined faults following rupture- and fracture-related increases in fault-parallel permeability. Decreases in fluid temperature and pressure along the flow path may then lead to significant increases in silica supersaturation. These increases in supersaturation, however, are to some extent counteracted by exponential decreases in kinetics associated with fluid cooling along the flow path. As such, the rates of quartz cementation and healing during fluid advection in nature are likely a complex function of fluid flux (both the rate and volume of advection) and the length scales of transport, bearing in mind that if advection leads to silica supersaturation and quartz precipitation then the ensuing cementation will reduce permeability, fluid flux, and transport length scales. The silica mass contributing to cementation is also, by definition, derived externally from the site of precipitation during advection-related cementation. The idea that the general mechanism of quartz precipitation in faults during upward advection occurs in nature is supported by geochemical analyses that show many fault-hosted quartz-gold deposits to have precipitated from fluids equilibrated with an external source (Beaudoin & Pitre, 2005; Bohlke & Kistler, 1986; Nesbitt et al., 1989). Several such deposits can be interpreted as injection-driven, where episodic injection of overpressured fluids drive swarms of relatively small ($M < 5$) earthquakes in low-permeability rocks (Cox, 2005, 2016). In some scenarios, fluids may exploit fault-localized permeability to descend to deeper crustal levels (e.g., Lin et al., 2003), potentially leading to relative increases in fluid temperature and pressure, undersaturation, and subsequent mineral dissolution. In this discussion, we focus on the role of upward fluid migration given its potential to facilitate quartz cementation.

Sibson (1989, 1992) was the first to describe a link between post-seismic fluid flow, cementation, and fault healing, arguing that cements may be both cause and consequence of the seismic cycle. This influential work prompts a number of questions regarding the magnitudes of supersaturation that may occur during post-seismic fluid flow, the length scales required to achieve them, and changes in kinetics as temperatures decrease along the flow path. To assess the effects of increased supersaturation on quartz precipitation rates during upward fluid flow, we calculate the solubility change associated with vertical fluid flow over 1–5 km length scales throughout the seismogenic crust. We then combine those supersaturations with the equations of Rimstidt and Barnes (1980) assuming that thermal equilibrium is maintained between migrating fluids and wallrock during upward flow (i.e., a "package" of fluid migrating from 15 to 10 km depth has a temperature broadly consistent with the geothermal gradient at 10 km depth on arrival). This assumption represents a maximum temperature change and therefore maximum potential supersaturation. We also assume that fluid flux is, in effect, infinitely fast, and thus that there is no time lag between the onset of fluid flow and cementation and no silica is lost from solution along the flow path. Although none of these assumptions are reasonable when applied to a real physical system, they have the effect of presenting a "best case" scenario regarding rates of quartz cementation and their ability to facilite fault and fracture sealing. Their implications will be discussed in detail below.

Figures 7a and 7b show calculated supersaturation and quartz precipitation rates during vertical fluid flow along faults at geothermal gradients appropriate for continental crust (~30°C/km) and subduction zones (~15°C/km), respectively. In both cases, a pressure decrease results from upward flow along fluid pressure gradients that are estimated to be near lithostatic (26.2 MPa/km). Supersaturations are generally less than 5 when assuming vertical fluid flow distances of 5 km, and less than 2 assuming vertical distances of only 1 km. The effect of supersaturation on quartz precipitation rates is always subordinate to that of temperature, and rates generally decrease exponentially with decreasing temperature/depth in the crust regardless of the length scale of vertical fluid flow. At any particular depth in the crust, however, the length scale of fluid transport has a substantial effect on the degree of supersaturation, and therefore on estimated quartz precipitation rates. At 10 km depth in continental crust, for example, the precipitation rate expected following vertical fluid flow from 15 km depth is nearly one order-of-magnitude larger than that expected following flow from 11 km depth. This is also true in the subduction zone example (Figure 7b), although the magnitude of the effect is slightly smaller due to the relatively smaller change in temperature (and therefore solubility) along the assumed flow path. Time scales of fracture healing estimated from our calculations vary from a few weeks to hundreds of thousands of years depending on temperature/depth, the length scale of fluid transport, and the assumed fracture aperture (Figures 7c and 7d). At 10 km depth in continental crust, for example, a fracture with a 10 μm aperture may seal in as little as 2 weeks during upward fluid flow from 15 km depth, or 4 months during fluid flow from 11 km depth. Alternatively, a fracture

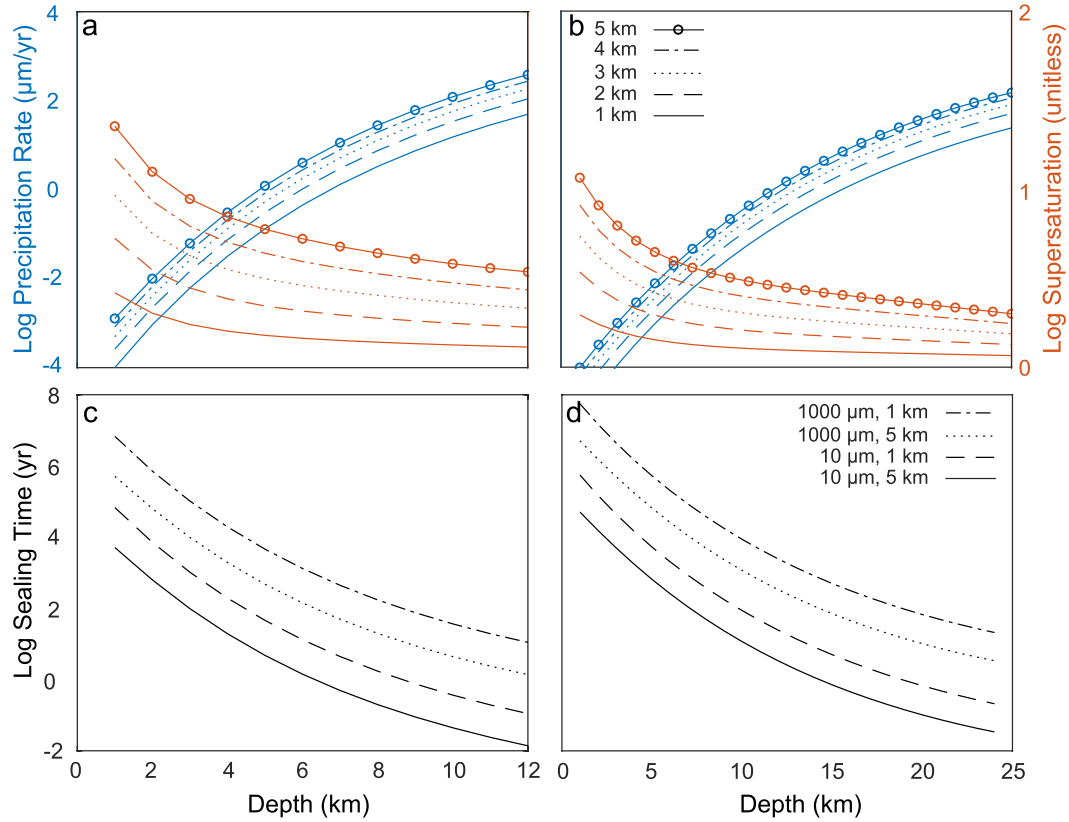

Figure 7. Plots showing estimated supersaturation and quartz precipitation rates (a and b) and fracture sealing/healing times (c and d) during upward fluid flow along vertical faults. Plots on left provide estimates for faults in continental crust (geothermal gradient = 30°C/km). (a) Supersaturation (red, secondary axis) and precipitation (blue, primary axis) rates estimated for faults in continental crust (geothermal gradient = 30°C/km). Line symbology denotes estimates for fluid flow from 1 to 5 km depth beneath a depth indicated on the *x* axis. Panel (b) same as panel (a), but for subduction zones (geothermal gradient = 15°C/km). (c) Estimated time scales of closure during quartz cementation for fractures with 10 and 1,000 μm apertures in continental crust. Line symbology denotes assumed aperture and length-scale of upward fluid flow as depicted in legend in panel(d). Panel (d) same as panel (c), but showing estimates of fracture closure time scales for subduction zones.

with a 1 mm aperture seals over a period of ~4.5 years during fluid flow from 15 km depth, or ~35 years during fluid flow from 11 km depth. Predicted sealing times increase exponentially with decreasing depth in the crust, such that sealing a 1 mm aperture fracture becomes unrealistic over typical interseismic intervals at depths shallower than ~5 and 10 km in continental crust and subduction zones, respectively.

2.2.1. Limitation and Caveats

Our calculations make several assumptions in estimating potential rates of quartz precipitation during upward fluid flow. One of the most fundamental is that the estimated length scales of fluid flow can be initiated and maintained indefinitely at all depths in the seismogenic crust. Upward fluid flow over multi-kilometer scales has been demonstrated in faults previously (e.g., Boles et al., 2015; Eichhubl & Boles, 2000; Newell et al., 2015; Williams, Beard, et al., 2019; Williams, Goodwin, et al., 2015), but most of these studies were focused on faults in the uppermost few kilometers of the crust. At these depths, brittle deformation leads to substantial increases in fault-zone permeability relative to protolith (e.g., Caine et al., 1996; Evans et al., 1997; Sibson, 1996), and provides the potential for significant mass flux that may not be possible at greater depths. As such, substantial volumes of fluid involved in large-scale advection are far more likely within networks of discrete fractures in fault damage zones than in cataclasites or other low-permeability materials localized along fault surfaces. Also, precipitation rates are slow at shallow depths, and permeability is therefore easier to maintain. Near the base of the seismogenic crust, however, upward fluid movement over multi-kilometer scales would by definition require substantial volumes of fluid derived from, and transported through, low-permeability rocks and shear zones in the underlying

ductile crust while maintaining said permeability. Large scale upward fluid migration from near the base of the seismogenic zone was inferred from geophysical observations immediately after the *Mw* 8.0 Antofagasta earthquake of 1995 (Husen & Kissling, 2001), but the amount of resultant quartz precipitation (if any) cannot be determined from these data. Although mass balance constraints from shear-zone-hosted ore deposits indicate that fluid transport over long distances is possible during ductile deformation (Cox, 2005), the rates and volumes of fluid movement are likely modest over interseismic time scales as fractures close. We note, however, that the syndeformational permeability of ductile shear zones may be larger than that measured in outcrop if permeability generation occurs by creep cavitation during local viscous grain boundary sliding (Fusseis et al., 2009; Menegon et al., 2015), or where interconnected, transgranular microcracks form at low effective stress (as demonstrated experimentally by Zhang et al., 1994). Regardless, low fluid-flow velocities imply that the time scales required to establish multi-kilometer-scale flow pathways at the base of the seismogenic crust likely exceed hundreds of years, broadly equivalent to the length of typical interseismic periods observed in many active faults. In this way, there may be a significant time lag between fault rupture and the onset of advection-related cementation, and it is therefore reasonable to treat the estimated time scales of fracture sealing in Figure 7c as minimum values. In particular, values estimated for near the seismic-aseismic transition, assuming upward fluid flow over several km, are likely to greatly underestimate the time scales of quartz cementation if fluid flux is limited by low permeability and limited fluid reservoirs. Some exceptions may occur locally within faults where, for example, injection of overpressured pore fluids leads to fluid-driven fracturing and faulting dominated by dilation (Cox, 2016). In the specific example of the European Union's Enhanced Geothermal System test site near Soultz-sous-Forêts, France, where fluids were injected into granite at 3.5 km depth, permeability increased from 10^{-17} to 10^{-14} m^2 (Evans et al., 2005), leading to fluid flow rates approaching meters per second (Cox, 2016).

In addition to considerations of the spatial and temporal scales of fluid transport, it is also important to recognize that our calculation does not account for potential changes in the concentration of SiO_2 in solution due to precipitation along the inferred flow path. Rimstidt and Barnes (1980) estimate that quartz precipitation rates likely reach a maximum value when solutions are cooled by ~50°C, corresponding to vertical length scales of only ~1.5 km in continental crust. Changes in fluid SiO_2 concentrations due to precipitation over a multi-kilometer vertical flow path are therefore expected, and indeed form the basis of the silica pore-fluid geothermometer (Fournier & Potter, 1982a). Thus, the silica supersaturations (and thereby quartz precipitation rates) estimated in Figures 7a and 7b are maximum values leading to minimum estimates for sealing time in Figures 7c and 7d, particularly at greater depths in the seismogenic crust where reaction kinetics are comparatively fast. A related factor not accounted for in our calculations concerns the availability of SiO_2-supersaturated fluids throughout the seismic cycle. In most crustal environments, it is unlikely that the concentration of dissolved SiO_2 exceeds 10^3 mg/kg water (Dolejš & Manning, 2010; Manning, 1994). Thus, the mass of SiO_2 dissolved in any unit volume of water is relatively small, and the maximum amount of quartz that can precipitate is limited to the difference between the concentration of SiO_2 in solution and that expected at equilibrium. Recognizing these facts, several previous efforts have estimated the fluid-rock mass ratios during quartz vein formation to be on the order of 10^3–10^4 or higher (Cox et al., 1991; Vrolijk, 1987a). As such, even small fractures with micron-scale apertures would require 10s of cubic meters of fluid to seal completely. It is worth noting, however, that many hydrothermal vein systems hosted in relatively small faults (i.e., displacement <1 km) inferred to have formed during fluid-driven earthquake swarms are highly localized. Recent calculations by Cox (2016), for example, imply total fluid volumes of 10^{-1}–10^0 km^3 over the 10^4–10^5 year lifespan of a fault-hosted quartz-gold deposit. Assuming repeat times between swarms of ~100 years, these estimates indicate fluid volumes of 10^5 m^3 per slip event, which are generally compatible with fluid production in magmatic or prograde metamorphic hydrothermal systems (Cox, 2016; Pitcairn et al., 2014). Sealing of larger faults typified by tectonically-driven, mainshock-aftershock sequences, however, would require larger fluid volumes to be distributed over a wider fault area than what is seen in relatively localized gold-quartz deposits. Thus, substantial volumes of fluid are required to facilitate quartz cementation over broad areas in plate-boundary faults, implying that post-seismic flow regimes must be maintained over periods of months, if not decades or hundreds of years in those systems. Some direct and theoretical constraints have demonstrated that post-seismic fluid discharge may indeed be maintained over these time scales (e.g., Braun et al., 2003; Williams, Beard, et al., 2019). It is likely, however, that in the case of maintained flow, the fluid pressure gradient over the full cementation period may be less than lithostatic, meaning that pressure changes during flow are smaller than those estimated in Figure 7. Similarly, rapid rates of fluid ascent along fault zones may lead to fault-localized thermal anomalies that reduce the magnitude of temperature decrease along

the flow path (e.g., Louis et al., 2019). These factors indicate again that the sealing times estimates presented in Figures 7c and 7d are necessarily minimum values that are only conceivable in high-flux, localized, hydrothermal systems.

Finally, it should also be noted, that if upward fluid flow is a requirement for quartz cementation and healing in faults, then comparatively rapid cementation at greater depths in the seismogenic crust may preclude significant cementation at higher structural levels by effectively destroying the permeability of the flow path during fracture sealing. Thus, the availability of SiO_2-supersaturated fluids may result in discontinuous sealing with depth in faults.

2.3. Rates of Quartz Precipitation Following a Decrease in Fluid Pressure

Decreases in pore-fluid pressure leading to silica supersaturation are also possible in the absence of upward fluid advection where fault deformation leads to dilation and permeability increase in overpressured sections of the crust. A critical difference between decreases in pore-fluid pressure due to advection and those due to dilation is that the latter may occur under isothermal conditions given the thermal mass and surface area of the surrounding wall rock (Weatherley & Henley, 2013). Thus, silica supersaturations may increase during slip without the corresponding decrease in the kinetic rate constant experienced during upward advection and cooling. In this scenario, quartz precipitation rates are governed principally by temperature and the magnitude of pore-fluid pressure drop. Much previous work has examined these processes as they relate to the precipitation of quartz cements in faults (e.g., Amagai et al., 2019; Nishiyama et al., 2020; Saishu et al., 2017; Sibson, 1982; Ujiie et al., 2018; Williams, 2019).

Two different mechanisms leading to coseismic decreases in fluid pressure have been discussed in the literature. The first considers the effect of coseismic increases in fault-zone permeability that lead to the re-establishment of hydraulic connectivity between an overpressured domain and the overlying hydrostatic crust (e.g., Sibson, 1992). In this case, the decrease in pore-fluid pressure during slip is limited to the difference between the lithostatic and hydrostatic pressures for a given depth (hereafter referred to as ΔP_{L-H}). This assumes that fluid overpressures consistent with the lithostatic load can be contained before slip, which is more likely in thrust/reverse fault settings where the least stress is vertical, than in strike-slip or normal faulting settings where the least stress is horizontal (Sibson, 2003). When assuming lithostatic and hydrostatic gradients of 26.2 and 9.8 MPa/km, respectively, ΔP_{L-H} can exceed several 100 MPa near the base of the seismogenic crust. It is likely, however, that this decrease is transient, as the re-establishment of hydraulic connectivity with the hydrostatic crust along faults will result in fault-localized, upward fluid advection and establishment of a more uniform pressure gradient. Decreases in pressure achieved in this way are therefore difficult to deconvolve from the effects of fluid advection discussed above. The remainder of this discussion will focus on coseismic decreases in fluid pressure induced by isolated dilational deformation and corresponding fluid decompression.

Dilational deformation can occur in isolated patches along faults during slip, caused by geometrical irregularities (e.g., Figure 1) and leading to highly localized fluid pressure decrease (e.g., Brantut, 2020; Sibson, 1987; Weatherley & Henley, 2013). As such, coseismic decreases in fluid pressure may occur without re-establishing hydraulic connectivity between overpressured horizons and the overlying hydrostatic crust. In this case, precipitation triggered by depressurization will occur from locally-derived fluids, in contrast to advection where fluids may be transported a substantial distance prior to precipitation. Thus, the magnitude of pressure change may, potentially, exceed ΔP_{L-H}. Theoretical and experimental constraints, for example, have shown that pore-fluid pressures may decrease from near-lithostatic to sub-MPa levels during coseismic dilational deformation along faults (e.g., Brantut, 2020; Weatherley & Henley, 2013). Pressure changes of this magnitude may result in local vaporization of pore fluids (i.e., "coseismic boiling") and potentially rapid precipitation of amorphous silica or other phases (e.g., Amagai et al., 2019). Recent work by Williams (2019), however, demonstrated that the mass of pore fluid that can be vaporized by slip-induced dilation is limited by rapid equilibration of vapor pressures (i.e., the pressure at which liquid and vapor phases are in equilibrium at a given temperature). The vaporized mass is too small for associated silica precipitation to seal more than 0.005% of the dilational volume with quartz.

To assess and isolate the effects of increased supersaturation on quartz precipitation rates during slip-induced dilation, we calculate the solubility change associated with sudden isothermal drop in fluid pressures at depths throughout the seismogenic crust. As in the previous section, we then combine those supersaturations with the

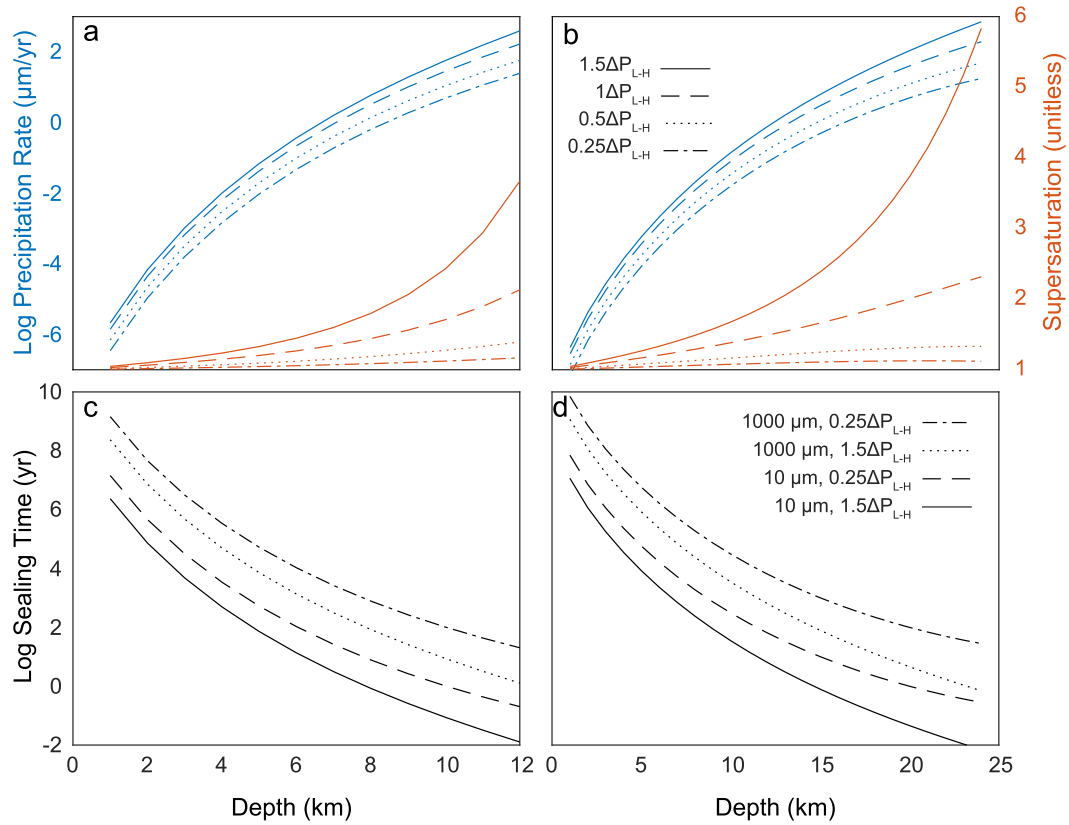

Figure 8. Plots showing estimated supersaturation and quartz precipitation rates (a and b) and fracture sealing/healing times (c and d) during coseismic decreases in pore-fluid pressure at a constant temperature. Plots on left provide estimates for faults in continental crust (geothermal gradient = 30°C/km). (a) Supersaturation (red, secondary axis) and precipitation (blue, primary axis) rates estimated for faults in continental crust (geothermal gradient = 30°C/km). Line symbology denotes simulated pressure drop magnitude as a factor of ΔP_{L-H} (the difference between the lithostatic and hydrostatic pressure at a given depth). Panel (b) same as panel (a), but for subduction zones (geothermal gradient = 15°C/km). (c) Estimated time scales of closure during quartz cementation for fractures with 10 and 1,000 μm apertures in continental crust. Line symbology denotes assumed aperture and pressure drop magnitude as depicted in legend in panel (d). Panel (d) same as panel (c), but showing estimates of fracture closure time scales for subduction zones.

equations of Rimstidt and Barnes (1980) to estimate rates of quartz precipitation. We consider slip-induced pressure decreases across a range of values above and below ΔP_{L-H}, but none that are sufficiently large to result in coseismic boiling as the volume precipitated during boiling is necessarily limited, as shown by Williams (2019). Although theoretical constraints indicate that meter-scale dilational volumes are required to induce pore-fluid pressure decreases large enough to appreciably impact silica solubility, more recent work has shown that these decreases may also be achieved during microfracturing in centimeter-scale deformation experiments (Brantut, 2020). As such, variations in supersaturation in response to coseismic decreases in pore-fluid pressure may potentially contribute to cementation of cataclasites and other low-permeability materials along fault interfaces as well as cementation of larger, discrete fractures in the surrounding damage zones.

Figures 8a and 8b show the results of supersaturation and quartz precipitation rate calculations for slip-induced dilation and associated decreases in pore-fluid pressure along continental and subduction zone thermal gradients, respectively. In both cases, pre-failure pore-fluid pressures are estimated to be near lithostatic (26.2 MPa/km). Decreases in fluid pressure during failure are then calculated as a factor of ΔP_{L-H} for a given depth assuming lithostatic and hydrostatic gradients of 26.2 MPa/km and 9.8 MPa/km, respectively. Supersaturations are generally less than 3 throughout most of the seismogenic crust when assuming a coseismic pressure drop of ΔP_{L-H}, and less than 1.5 when considering a smaller pressure drop of $0.5\Delta P_{L-H}$. Larger pressure drops of $1.5\Delta P_{L-H}$ may produce supersaturations up to 3.5 or 6 in continental crust and subduction zones, respectively. The effect of depressurization on supersaturation and quartz precipitation rates, however, decreases with decreasing depth/temperature

in the crust, a result of the decreased role of fluid pressure in determining silica solubility at low temperatures (e.g., Figure 5). The effect is also generally larger in subduction zones, owing to the reduced geothermal gradient and therefore larger pre-failure fluid pressures (and therefore ΔP_{L-H}) at seismogenic depths. Similar to the results of fluid advection calculations, estimated time scales of fracture healing during coseismic depressurization vary from a few days to hundreds of thousands of years depending on temperature/depth, magnitude of pressure decrease, and the assumed fracture aperture. At 10 km depth in continental crust, for example, a fracture with a 10 μm aperture may seal in as little as 4 weeks following a pressure drop of $1.5\Delta P_{L-H}$, or 1 year following a pressure drop of $0.25\Delta P_{L-H}$. Alternatively, a fracture with a 1 mm aperture seals over a period of 9 years following a pressure drop of $1.5\Delta P_{L-H}$, or 100 years following a pressure drop of $0.25\Delta P_{L-H}$. Also similar to results of our fluid advection calculations, sealing times increase exponentially with decreasing depth in the crust, such that sealing a 1 mm aperture fracture becomes unrealistic over typical interseismic intervals at depths shallower than 7 and 16 km depth in continental crust and subduction zones, respectively.

2.3.1. Limitations and Caveats

The above calculations depend on several assumptions which are unlikely to be satisfied in nature. The most basic of these assumptions is that the estimated pressure drop magnitudes are reasonable during faulting. Theoretical constraints indicate that coseismic decreases in fluid pressure may locally exceed several 100 MPa (e.g., Weatherley & Henley, 2013). There is, however, relatively little direct evidence to indicate that pressure drops of this magnitude actually occur during earthquakes in the crust. Parry and Bruhn (1990) examined CO_2-rich fluid inclusions in quartz from the Wasatch fault, USA and inferred pressure transients of 125 MPa near the base of the continental seismogenic crust ($0.75\Delta P_{L-H}$). Ujiie et al. (2018) inferred coseismic decreases in fluid pressure of up to 235 MPa during micro-slip events based on observations of fluid inclusions in quartz slickenfibers from the exhumed Makimine accretionary complex, Japan. Broadly similar pressure drops were inferred on the basis of fluid inclusion studies by Vrolijk (1987b) in the Kodiak accretionary complex, Alaska, USA. Other direct support for coseismic decreases in pore-fluid pressure more generally is available in the form of "implosion" breccia observed within some exhumed fault jogs. These breccia, however, require a tensile normal stress to develop along the fault, and as such they may be a rare occurrence restricted to faults that have sufficient cohesion for substantial fluid overpressures to develop before fault reactivation occurs (Sibson, 1986). More recent research by Fisher et al. (2019) argued that coseismic pressure drops in microfractures are on the order of no more than a few 10s of MPa, because they are limited by the tensile strength of the wall rock. Similarly, geophysical observations of *Vp*/*Vs* ratio before and after large earthquakes and episodic tremor and slip events indicate only modest variations in pore-fluid pressure (a few 10s of MPa) following rupture (Gosselin et al., 2020; Husen & Kissling, 2001). The lack of support for coseismic decreases in pore-fluid pressure in the seismological record, however, could result from depressurization of local volumes below the resolution of seismological observation (a few 10's of m), which is consistent with theoretical and experimental data (e.g., Brantut, 2020; Weatherley & Henley, 2013). A related assumption implicit within our calculations is that the estimated pressure drop magnitudes (if achievable) are sustainable over the time scales required to seal faults and fractures with quartz cements. Few data are available to estimate the time scales of pressure recovery following slip-induced dilation in the crust, although they are likely proportional to the magnitude of initial pressure decrease, the total volume of the depressurized zone, and the permeability of the surrounding wall rocks. For cm^3-scale dilational volumes, recent experimental results show that pore-fluid pressures may recover to pre-failure levels within a matter of minutes (Brantut, 2020). Additional constraints are required to estimate the longevity of low pressure regions within fault zones following earthquake rupture.

A more fundamental limitation to the rate and volume of quartz cements formed in response to coseismic decreases in pore-fluid pressure concerns the hydrology and mass balance implied by the mechanism of depressurization. Williams (2019) argued that coseismic decreases in pore-fluid pressure resulting from dilational deformation alone (as opposed to those caused by re-establishment of hydraulic connectivity between the previously overpressured volume and the overlying hydrostatic crust) result in highly underpressured volumes within fault zones. These underpressured volumes are by definition surrounded by wallrocks with pore-fluid pressures comparable to pre-failure values. Thus, the hydraulic gradient is uniformly directed inward toward the underpressured volume(s), and the maximum volume of fluid that can be moved across that gradient is the amount required to (re)fill and (re)pressurize the dilational space. Stated alternatively, large decreases in pore-fluid pressure that are during coseismic dilational deformation cannot occur in conjunction with fluid transport over distances much farther than the length scales of the dilational volumes. As discussed in the previous section, however, the

fluid-rock mass ratios required during quartz precipitation are likely on the order of 10^3 or higher, suggesting that coseismic decreases in pore-fluid pressure alone are likely not be capable of producing appreciable volumes of quartz cement.

Given the above considerations, the volume of quartz cement that may form in response to depressurization can be represented as a percentage of the dilational volume by calculating the amount of quartz that forms per unit volume of depressurized water. At 10 km depth in continental crust under lithostatic pore-fluid pressure conditions (pre-failure conditions ~300°C and ~260 MPa), for example, a large coseismic pressure decrease of $1.5\Delta P_{L-H}$ results in a decrease in the solubility of SiO_2 from ~775 mg SiO_2/kg water to ~320 mg SiO_2/kg water (Figure 5; Manning, 1994). The maximum mass of quartz that can form in response to this change is therefore ~450 mg/kg of depressurized water. It is important to note that this estimate is necessarily a maximum value, as precipitation rates will asymptotically approach zero during precipitation in a closed system (see equations above). Assuming a quartz density of 2.65 g/cm^3, 450 mg of SiO_2 precipitated as quartz occupies a volume of 0.2 cm^3. At 300°C and <50 MPa fluid pressure, the specific volume of water is ~775 kg/m^3. A coseismic pressure drop of $1.5\Delta P_{L-H}$ near the base of the seismogenic continental crust may therefore produce ~155 cm^3 of quartz cement per m^3 of water depressurized. Given that the maximum fluid flux possible into an underpressured dilational volume is broadly comparable to that volume, this calculation also provides an estimate of the amount of quartz that may form per m^3 of coseismic dilation within faults. Thus, coseismic decreases in pore-fluid pressure near the base of the seismogenic continental crust are unlikely to result in sealing of more than 0.02% of the dilational volume formed during slip. When this same calculation is applied to failure in a subduction zones at 24 km depth, we find that coseismic decreases in pore-fluid pressure may seal up to 0.05% of the dilational volume. When assuming dilational sites that are completely filled with fluid, our calculations are effectively normalized to the dilational volume formed during slip. As such, they apply equally to nm-to-μm-scale microfractures in cataclasites lining fault surfaces as they are to larger mm-to-m scale fractures and breccia in fault damage zones (or meter-scale dilational jogs along fault surfaces; i.e., Weatherley & Henley, 2013). In summary, the rates of quartz precipitation associated with coseismic decreases in pore-fluid pressure may be substantial when the pressure change is sufficiently large, but the overall volume of quartz precipitated is unlikely to seal fractures and affect fault mechanics. This limitation is an effect of the relatively small amount of silica that can be dissolved in water prior to failure, and the need for a local silica source for rapid precipitation in response to depressurization. In advective systems, this limitation is less relevant, but instead, fault-parallel fluid flow will cause recovery of fluid pressure in dilatant sites, and negate the supersaturation effect of co-seismic pressure drops.

2.4. Frictional Heating

Frictional heating during shear at coseismic slip rates can result in temperature transients capable of melting rocks along a fault interface (i.e., pseudotachylytes; e.g., Goodwin, 1999; Kirkpatrick et al., 2012; Rowe et al., 2018; Sibson et al., 1975). These transients, although profound, are highly localized to a volume immediately adjacent to the fault surface, and generally decay to pre-failure levels through thermal diffusion over time scales of hours to a few days (Cardwell et al., 1978; Lachenbruch, 1986). Thus, it is reasonable to assume that SiO_2 solubility and kinetics are greatly affected over similar spatial and temporal scales. In this section, we focus on the effects of frictional heating that potentially lead to quartz cementation, although it is likely that other mechanisms such as sintering or dissolution-precipitation creep would also contribute significantly to healing at high temperatures following slip.

As mentioned previously, SiO_2 solubility is dependent on both temperature and the specific volume of water (Manning, 1994), the latter depending on both temperature and pressure (Wagner & Kretzschmar, 2008). Assuming a constant pressure, increasing temperature results in an increase in the solubility of SiO_2 up to a local maximum where the effects of increasing specific volume begin to counteract temperature in increasing solubility. In practice, increasing specific volume will be counteracted during frictional heating, as temperature and pressure likely rise in concert due to the effects of thermal expansion and pressurization during coseismic slip (O'Hara et al., 2006; Rempel & Rice, 2006; Wibberley & Shimamoto, 2005). Solubility should therefore increase directly with frictional heating up to the melting point of the fault rocks. The exponential dependence of SiO_2 kinetics on temperature also suggests that frictional heating is likely accompanied by rapid, localized dissolution along the fault interface and perhaps in the immediately adjacent damage zone during thermal diffusion. Subsequent cooling to pre-failure temperatures may then lead to supersaturation and increased rates of quartz precipitation. As an

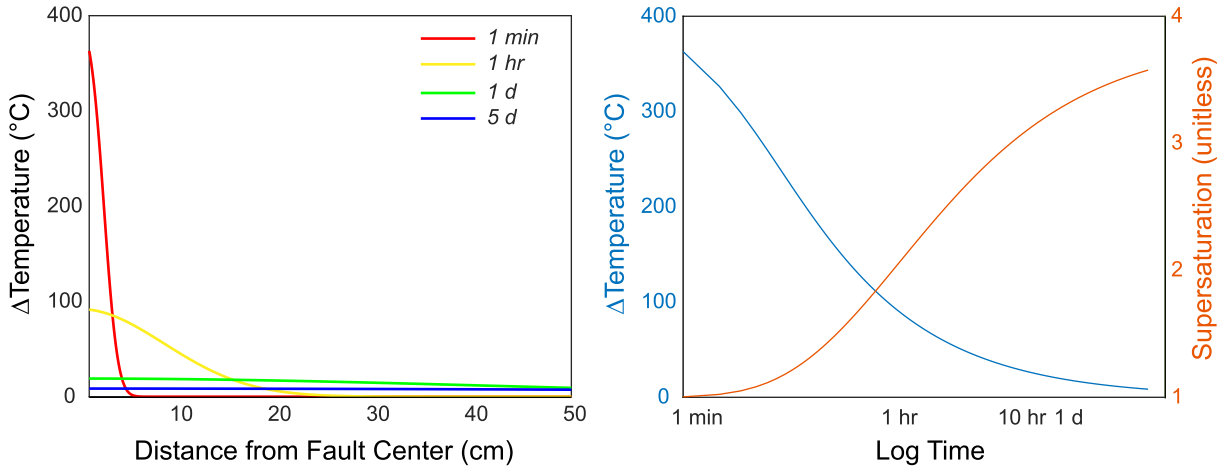

Figure 9. (Left) Profiles of temperature change above pre-failure (300°C) values as a function of distance from the fault center. (Right) Profiles displaying change in on-fault temperature (blue, left) and SiO_2 supersaturation (red, right) as a function of time following failure assuming SiO_2 equilibrium is achieved during peak temperatures immediately following slip.

example, we consider the magnitude of SiO_2 solubility change associated with isobaric frictional heating during a seismic (i.e., m/s) slip event. Using the equations of (Lachenbruch, 1986), we assume a coseismic displacement of 1 m occurring over a duration of 1 s on a shear zone 5 cm in thickness at 10 km depth in continental crust (i.e., pre-failure conditions ~300°C and 260 MPa). Fault normal stress is assumed to be ~50 MPa, and the density and heat capacity of the fault rocks are assumed to be 2.65 g/cm^3 and 0.95 J g^{-1}°C^{-1}, respectively. Using this formulation, on-fault temperatures immediately after rupture approach ~700°C, but fall to ~400°C within the first hour post-failure (Figure 9). On-fault temperatures are estimated to be within 20°C of pre-failure values after 24 hr. Assuming equilibrium is achieved quickly at maximum temperature due to increased SiO_2 kinetics and thereby rates of dissolution (e.g., Dove & Rimstidt, 1994), the concentration of SiO_2 in solution prior to post-slip cooling would be ~3×10^3 mg/kg (Manning, 1994). The equilibrium concentration of SiO_2, however, decreases rapidly as temperatures dissipate, resulting in supersaturations in excess of three within the first 8 hr post-failure. The limited temperature range of the (Rimstidt & Barnes, 1980) calibration prevents us from estimating quartz precipitation rates throughout post-seismic cooling. It does appear, however, that coseismic frictional heating and subsequent cooling is likely capable of producing supersaturations and quartz precipitation rates in excess of those experienced during km-scale fluid advection or coseismic decreases in pore-fluid pressure, but with a silica source that is limited to less than ~10 cm from the fault and therefore very small.

Experiments reported by Rowe et al. (2019) show frictional heating at coseismic slip rates may also produce significant quantities of amorphous silica lining the slip surfaces in quartz-rich fault rocks. The production of these phases is not attributed to direct precipitation from solution, but rather a combination of frictional heating, mechanical wear, and the availability of fluids hydrating the surface of comminuted particles. As discussed by Rowe et al. (2019), post-seismic dehydration reactions in hydrous amorphous silica phases may contribute to fault healing through a process akin to recrystallization. This process likely occurs over time scales of a few years at temperatures reflective of the seismogenic crust (Bettermann & Liebau, 1975). Other experimental work by Williams, Farver, et al. (2015), however, demonstrates that 10 μm microfractures in quartz grains adjacent to an amorphous silica layer may heal in as little as 1 week at 300°C. Raman spectrometry also revealed that healing in the Williams, Farver, et al. (2015) experiments was driven by dissolution of the amorphous silica and subsequent reprecipitation as α-quartz in microfractures, suggesting that these combined reactions may result in sealing of thin, discrete fault surfaces over time scales considerably faster than those anticipated for recrystallization alone.

2.4.1. Limitations and Caveats

Quartz cementation resulting from frictional heating and subsequent cooling suffers from a significant mass balance limitation. The maximum volume of quartz precipitated during cooling cannot exceed that originally dissolved during heating (i.e., no SiO_2 mass is added to the fault zone locally). Thus, quartz precipitation driven by frictional heating and subsequent cooling is highly localized both spatially and temporally, and cannot contribute

to large abundances of quartz-cemented veins observed in the damage zones of some faults (e.g., Figures 2 and 3). Despite this limitation, cementation induced by frictional heating and subsequent cooling still has the potential to significantly alter fault strength by effectively mobilizing and redistributing silica in the immediate vicinity of the slip surface, potentially rebonding broken grains and increasing fault strength. This process can explain thin silica cements sealing some limited segments of natural faults (Faber et al., 2014; Kirkpatrick et al., 2013). Stated alternatively, it is likely that this mechanism yields a limited volume of quartz cement, but those cements are also likely to precipitate on the primary slip surface where they would have the most dramatic effect on mechanics. Moreover, the effect of this redistribution on fault mechanics may be augmented when acting in conjunction with dissolution-precipitation creep and/or sintering at peak temperatures during frictional heating (e.g., Curewitz & Karson, 1999; Hirono et al., 2020; Tenthorey & Cox, 2006; Tenthorey et al., 2003).

The potential for quartz cementation to occur due to dissolution and reprecipitation of amorphous silica phases produced during frictional heating appears promising, particularly as experimental work has already validated the general mechanisms (e.g., Rowe et al., 2019; Williams, Farver, et al., 2015). A key parameter governing the efficacy of this process is the volume of amorphous silica produced during slip. Experiments conducted by Rowe et al. (2019) show that slip at coseismic velocities in quartz-rich materials consistently produced a 5–30 μm thick layer of amorphous silica. The volume of amorphous silica formed, however, increases with faster slip velocity for experiments of equal displacement. Thus, the potential for quartz cementation due to dissolution and reprecipitation of amorphous wear products is greatest following larger earthquake ruptures. Regardless of rupture size, however, the total volume of amorphous silica produced is unlikely to exceed a few 10s of μm thickness along the slip surface.

2.5. Dissolution-Precipitation Creep

Silica solubility and reaction kinetics may also vary at much more local (e.g., μm to sub-μm) scales than those documented above. For example, dissolution-precipitation creep is a well documented phenomenon in faults and other rocks whereby increased normal stress at grain-to-grain contacts results in a local increase in silica solubility and dissolution (Elias & Hajash, 1992; Rutter, 1983). Reprecipitation of quartz cements may then occur following diffusive mass transfer, typically in a fluid phase, to sites of relatively low normal stress and low solubility (i.e., precipitation occurs under slightly supersaturated conditions; Mullis, 1991). Unlike many of the mechanisms described above, the potential for cementation associated with dissolution-precipitation creep is influenced by a large variety of factors in addition to temperature and pressure. These may include the presence of phyllosilicates; fluid chemistry; grain-size, shape, and spatial configuration; and gradients in effective fault-normal stress (Bos & Spiers, 2000; Elias & Hajash, 1992; Giger et al., 2008; Houseknecht, 1984; Kanagawa et al., 2000; Niemeijer et al., 2008; Renard et al., 2000; Yasuhara et al., 2005), implying that dissolution-precipitation creep may contribute to quartz cementation both in nm-to-μm-scale microfractures in cataclasites (e.g., Tenthorey & Cox, 2006; Tenthorey et al., 2003) localized along fault surfaces and in cementation of larger, more discrete fractures and/or breccia in fault damage zones (e.g., Fisher et al., 2019). Many of these factors cannot be easily constrained, in part because they are likely to vary significantly as a function of depth, lithology, and stress state in the crust. Moreover, the effects of dissolution-precipitation creep on fault-rock healing extend beyond those associated with cementation, as dissolution at grain-to-grain contacts also results in an increase in real contact area between comminuted grains (e.g., Niemeijer et al., 2008; Yasuhara et al., 2005) and loss of permeability (e.g., Giger et al., 2007). Notably, Fisher et al. (2019) conducted a theoretical analysis incorporating these effects and suggested that dissolution-precipitation creep of quartz cements in nearby fractures may provide an effective mechanism for healing fault rocks over decadal time scales in subduction zones. The nature of their analysis, however, implies that the results are highly specific to the assumed lithologies (particularly grain size) and tectonic setting. The magnitude of healing due to dissolution-precipitation creep in quartz-rich rocks was explored by Tenthorey et al. (2003) and Tenthorey and Cox (2006), who showed experimentally that the combined effects of local dissolution and precipitation on fault-rock strength are profound, potentially recovering up to 75% of pre-failure strength over a period of only 6 hr in combined deformation and hydrothermal reaction experiments. These experiments, however, were conducted at temperatures in excess of 900°C to promote reaction at laboratory time scales. The fact that this process has proven difficult to reproduce in other laboratory experiments (e.g., Rutter, 1983) at lower temperatures suggests that at conditions typical of the seismogenic crust, healing related to dissolution-precipitation creep may occur over much longer time scales, perhaps on par with those concluded by (Fisher et al., 2019), or potentially longer. That dissolution-precipitation creep at

seismogenic temperatures is slow relative to high temperature experiments, but applicable at interseismic timescales, is supported by extrapolation of the results of Tenthorey et al. (2003) and Tenthorey and Cox (2006), which shows that as much as 100 MPa of cohesive strength recovery occurs in less than 10 years at 300°C. We also note that even without extrapolation, the original experimental conditions and rates utilized by Tenthorey et al. (2003) and Tenthorey and Cox (2006) are entirely reasonable for those that may be encountered during frictional heating, as described in the previous section.

2.5.1. Limitations and Caveats

Given that little is known about the absolute rates and efficacy of fault-healing related to dissolution-precipitation creep in nature, similarly little may be inferred regarding its limitations. One aspect of this process that is constrainable, however, suggests that similar to the effects of coseismic pressure drops and frictional heating, quartz cementation associated with pressure solution is unlikely to result in a net increase in the SiO_2 content of a fault zone. The diffusive mobility of silica is limited over interseismic timescales at conditions typical of the seismogenic crust (Watson & Wark, 1997). Moreover, microstructural and theoretical considerations of dissolution-precipitation creep suggest that reprecipitation commonly occurs in the immediate vicinity of dissolution (e.g., Gratier et al., 2013). As such, cementation associated with pressure solution suffers from a significant mass balance limitation, and likely cannot explain cementation of extensively cemented, quartz-vein rich damage zones observed in some faults (or at least not over interseismic timescales). Similar to the effects of frictional heating, however, pressure solution may act specifically in the vicinity of slip surfaces, suggesting that although associated cementation and contact-area spreading may be limited in magnitude, they may still exert a substantial control on the time-dependent strength of faults (Tenthorey & Cox, 2006; Tenthorey et al., 2003; Van den Ende & Niemeijer, 2019). Ultimately, more long term experiments may be required to improve our understanding of the rates of dissolution-precipitation creep and their impact on fault strength under seismogenic conditions.

2.6. Quartz Precipitation Driven by Variations in Fluid and Surface Chemistry

Variations in the chemistry of subsurface fluids and mineral-precipitation surfaces may also affect quartz precipitation rates during faulting. The mechanism by which these factors regulate quartz precipitation rates can generally be divided into two categories: variations associated with changing the equilibrium solubility of SiO_2 in solution (thermodynamic effects), and those associated with catalyzing reactions on mineral surfaces (kinetic effects).

In addition to temperature and pressure, the solubility of SiO_2 in aqueous fluids is also partially controlled by fluid pH, salinity, and composition (e.g., mixed phase H_2O-CO_2-CH_4-etc. fluids). Variations in these parameters during faulting may therefore result in increased supersaturation and associated quartz precipitation. Of these, the effects of pH and salinity on SiO_2 solubility are arguably the most well constrained. It is important to note, however, that the pH of water in contact with quartz-rich rocks is buffered to a maximum of ∼9.8 due to changes in the dissolved form of SiO_2 at larger values (Dove & Rimstidt, 1994). At this value, the solubility of SiO_2 is increased by a factor of ∼2 relative to that expected for a neutral solution at the same temperature and pressure. Salinity also exerts a control on SiO_2 solubility, but these effects are generally smaller than those associated with changes in pH. For example, the effect of NaCl concentration on SiO_2 solubility is comparatively negligible at temperatures less than 350°C for NaCl concentrations up to ∼10 wt% (a factor of ∼1.5; Newton & Manning, 2000). In solution with NaCl concentrations in excess of 10 wt%, the solubility of SiO_2 decreases with increasing salinity due to marked changes in the activity of water (a behavior sometimes referred to as "salting out"). Experiments have demonstrated that similar effects may decrease the solubility of SiO_2 in solutions with large fractions of dissolved volatiles such as CO_2 or CH_4 (Newton & Manning, 2000) which has been inferred to affect the propensity for quartz cementation and healing in some faults (e.g., Cook et al., 2006). Changes in SiO_2 solubility due to variations in the surface chemistry of solids have also been predicted on a theoretical basis and confirmed experimentally. For example, the solubility of SiO_2 experiences a marked decrease near crack tips and within nano-scale pores (Dove & Rimstidt, 1994; Wang et al., 2003), suggesting that precipitation rates at those scales may depart from those predicted based on the chemistry and supersaturation characteristics of the bulk fluid phase.

Variations in fluid chemistry may also have a catalytic effect on rates of quartz dissolution and precipitation even in the absence of significant variations in SiO_2 solubility. Unfortunately, the overwhelming majority of research in this area has focused on variations in the rates of quartz dissolution, largely due to difficulties in measuring

quartz precipitation over reasonable laboratory time scales. Thus, these effects can be only cautiously applied to processes occurring during quartz precipitation. In either case, the catalytic mechanisms affecting reaction kinetics are difficult to deconvolve from variations in SiO_2 solubility that share a similar origin. Fluid pH, for example, has been shown to increase the rates of quartz dissolution in both acidic and basic solutions. In the former, this rate increase may be caused in part by catalytic effects of pH change, or alternatively to larger undersaturations associated with increased SiO_2 solubility at relatively high pH. For acidic solutions, however, it is likely that this increased rate arises from catalysis alone, as the solubility of SiO_2 experiences negligible variations in this pH range (Fleming & Crerar, 1982). The catalytic effects of electrolytes are more clear, where NaCl in solution increases the rates of quartz dissolution and precipitation despite having a negligible (or negative) effect on SiO_2 solubility (Newton & Manning, 2000). Interestingly, catalysis of quartz dissolution and precipitation also exhibits a cation dependence, where the effects of Na are similar to those of K, which are greater than Li and Mg (Dove & Crerar, 1990; Hosaka & Taki, 1981). Of particular relevance to cementation in faults, recent experiments (Williams, Farver, et al., 2015) and comparisons of vein microstructures to numerical models of crystal growth (Spruženiece et al., 2021) have shown that surface chemistry effects may result in order-of-magnitude variations in quartz precipitation rates on freshly fractured surfaces when compared to the original grain boundaries. This effect is likely the result of fracturing producing precipitation sites that are anhedral and largely free of nucleation discontinuities such as phyllosilicates (Lander & Laubach, 2015; Lander et al., 2008). In this way, fractures that have apertures of sufficient width to allow for the formation of euhedrally-terminated quartz cements may experience a decrease in cementation rate during sealing (Lander & Laubach, 2015). This process, however, is unlikely to affect the cementation of microfractures in cataclasites, given the limited apertures observed in those structures (e.g., Milliken et al., 2005). Collectively, what is known about the controls of fluid and surface chemistry on quartz solubility and kinetics suggests that variations in these properties could result in both substantial increases and decreases in precipitation rate relative to those predicted above. In certain circumstances, these effects may result in discontinuous partial sealing or "bridging" of fractures with cement along their lengths, such as that documented in some faults at relatively shallow depths (Laubach et al., 2014), and in different vein populations at a range of depths (Fisher & Byrne, 1990). We note that the mechanical implications for such variations in vein-cement morphology (i.e., variations from open, to partially bridged, to completely sealed) are insufficiently described, largely unknown from a quantitative perspective, and likely represent a fruitful avenue for future experimental research. For a more complete discussion of fluid and surface chemistry effects, the reader is referred to the review by Dove and Rimstidt (1994).

2.6.1. Limitations and Caveats

The magnitude of variations in rates of dissolution caused by fluid and/or surface chemistry are up to an order of magnitude in scale and well constrained by experimental studies. How these parameters affect quartz precipitation rates are comparatively poorly understood. This paucity of empirical data is a source of substantial uncertainty and moreover, it is likely that the potential for these factors to influence rates of quartz dissolution or precipitation are dependent on the dynamics of fluid-fault interactions throughout the seismic cycle. For example, large variations in fluid chemistry are most likely where fluids from hydrologically and geochemically distinct aquifers experience mixing during fluid advection. Thus, variations in fluid chemistry may offer partial explanation for abundant quartz cements observed in mineral deposits related to anomalously high fluid fluxes in dilatant faults, such as in the Motherlode quartz-gold deposits in California, USA (Weir & Kerrick, 1987). Such examples of vein-rich fault zones are, however, not unique to mineralized systems, but can also occur in dilatant fault segments in non-mineralized settings (de Ronde et al., 2001; Eichhubl & Boles, 2000; Sibson, 1994, 2017). Ultimately, a substantial amount of additional empirical data are required before these effects can be fully understood, which may be obtained from a combination of laboratory experiments and detailed analysis of hydrothermal ore deposits and other high fluid flux, vein-rich fault systems.

3. Discussion

The above review of quartz cementation processes, rates, and limitations highlights that no single, currently understood mechanism can explain both aggregate quartz cementation of cataclasites along fault surfaces and sealing of larger, more discrete fractures in the surrounding fault damage zones over interseismic time scales (Table 1). The conclusions we can draw from the calculations do, however, vary with tectonic setting, and we will briefly discuss this—recognizing that some of this discussion was anticipated by Sibson (2003) and Sibson

Table 1
Summary of Potential Slip-Related Mechanisms for Increasing Silica Supersaturation, Supporting Evidence of Action in the Crust, and Efficacy With Respect to Fault Healing Over Interseismic Time Scales

	Geological evidence	Potential to seal veins fast enough to affect seismic cycle?	Potential to provide sufficient volumes of quartz to fill open faults and fractures?
Precipitation of metastable phases	Preserved microstructures of metastable precursors (e.g., flow banding, spherules, amorphous silica)	Only at shallow depths or during boiling/rapid depressurization	Only at shallow depths or during boiling/rapid depressurization
Post-seismic fluid advection	Geochemical signatures of external fluids	Yes, if sufficient supersaturated fluids are introduced—requires multi-km vertical transport at temperatures near the base of the seismogenic zone	Only if fluid flow and supersaturation can be maintained untill fractures are sealed
Co-seismic depressurization	Fluid inclusions in conjunction with geochemical signatures of local fluids	Yes, at temperatures near the base of the seismogenic zone	Generally no. May be feasible when acting in conjunction with advection to improve mass balance
Frictional heating	Presence of pseudotachylytes	Yes, but only for a short period following slip	Likely only sufficient to seal very small dilational sites with very local re-precipitation. Cannot explain large vein systems
Pressure solution	Local dissolution and precipitation microstructures	Possibly, depending on temperature and diffusive time scales—more likely if associated with frictional heating	Depends on diffusive distance, but likely to seal only very small dilational sites with local reprecipitation. Can explain large vein systems, but only over time scales much longer than typical interseismic periods
Variations in fluid/surface chemistry	Fluid inclusions, vein chemistry	Possibly—difficult to define and calculate	Possibly—dependent on fluid chemistry and supply

and Rowland (2003), and that cementation processes evolve with time and depend on pressure, temperature, and salinity (Monecke et al., 2018). We then attempt to reconcile our limited understanding of quartz cementation with its implications for fault-related processes on earthquake cycle time scales, followed by recommendations for future research.

3.1. The Role of Tectonic Setting

The potential for each of the above processes to control rates of quartz cementation and healing is dictated in part by tectonic setting, kinematics of faulting, and the orientations of the principal compressive stresses (see more complete discussion by Blenkinsop, 2008; Cox, 2010; Sibson & Rowland, 2003). For example, our calculations indicate that substantial volumes of fluid must migrate over kilometer-scales through faults in order for quartz to seal fractures more than a few μm thick over interseismic time scales during fluid advection (Figure 7). Observation of modern post-seismic fluid flow, however, suggests that at least at relatively shallow depths, these flow regimes are most readily achieved in seismogenic normal faults, where discharge volumes at the surface are up to 10 times greater than those resulting from similarly sized earthquakes in strike-slip or reverse systems (Muirwood & King, 1993). Little is known, however, about discharge volumes at greater depths in seismogenic faults, where host rock permeability is lower and the faults themselves may have transiently high permeability and be connected to overpressured reservoirs, parameters that may allow local and transient high flux flow. Previous geochemical analysis of fault-localized vein systems in a seismogenic normal fault indicate that the length scales of post-seismic fluid transport may exceed ~20 km in some circumstances (Williams, Beard, et al., 2019). Thus, it is likely that post-seismic fluid flow along normal faults involves significant changes in fluid temperature and pressure, in addition to maximizing the potential for mixing reactions that may influence fluid chemistry and precipitation. The former is promoted by the generally steep orientation of normal fault systems when compared to those observed in subduction thrust environments (Figure 10). Large changes in fluid temperatures would also be promoted during sub-vertical fluid flow through relatively high thermal gradients in rifts and other extensional

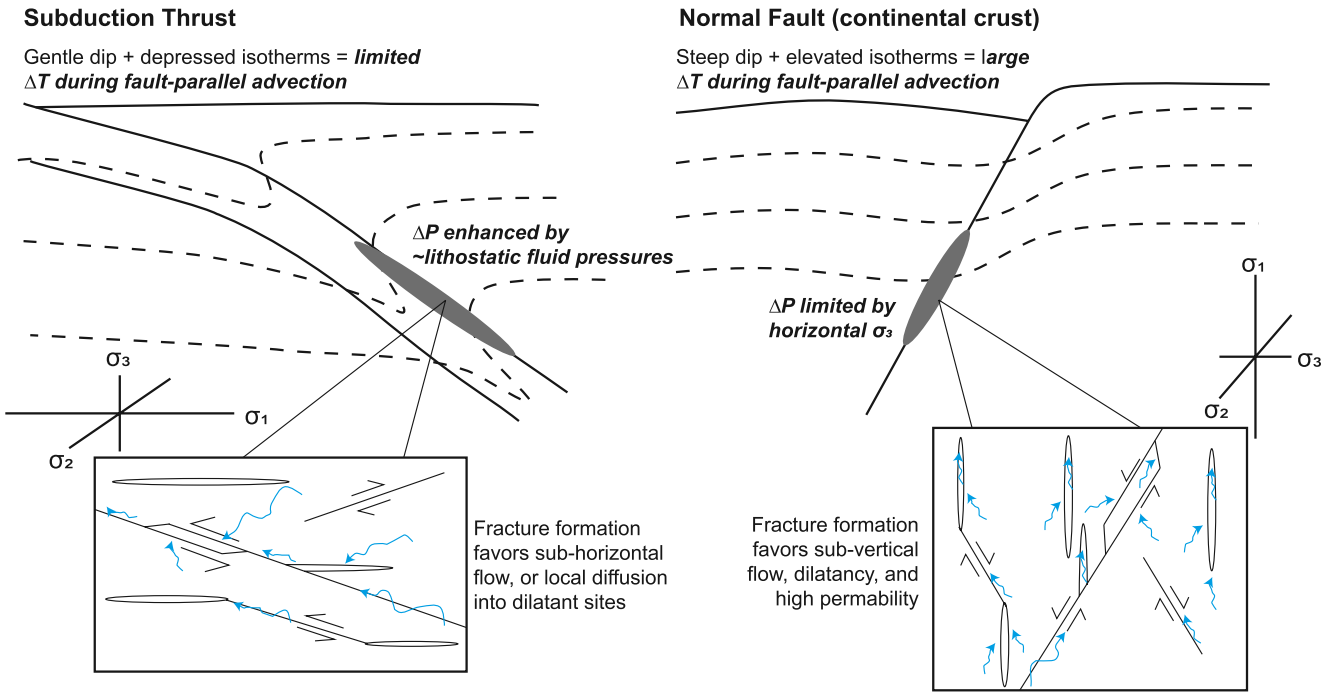

Figure 10. Schematic diagram illustrating contrasting fluid-advection and coseismic-pressure drop potential in subduction thrusts (left) and normal faults (right). Shaded ellipses depict areas of suprahydrostatic pore-fluid pressures at depth, which are inferred to be limited in magnitude to that of the least principle-compressive stress. Schematic fracture networks are those expected for the principle stress directions and magnitudes for each of the tectonic environments. The figure is inspired by Sibson (2003).

systems. We note that although these observations suggest that normal faults may be relatively favorable to quartz precipitation induced by fluid advection, similar processes are also likely in the vicinity of dilational jogs in strike-slip settings (e.g., Sibson, 1987), and advective flow may be promoted in any tectonic setting during transient flow coupled to failure driven by injected overpressured fluids (e.g., Cox, 2016). Ultimately, more empirical constraints are required to test these hypotheses.

Our calculations also show that coseismic variations in pore-fluid pressure may substantially affect rates of quartz cementation in faults, particularly where those variations are large in magnitude (Figure 8). It is reasonable then to conclude that the potential for quartz cementation due to pore-fluid pressure change is greatest where pre-failure pressures are largest (near the base of the seismogenic zone). As such, fluid pressure drops may be a particularly important mechanism of driving quartz precipitation in subduction zones, where earthquake nucleation depths routinely exceed 10s of km due to locally decreased geothermal gradients and the corresponding deepending of the base of the seismogenic zone. Moreover, maximum pore-fluid pressure is generally limited to the magnitude of the least principal stress at the time of failure, given the low tensile strength of rocks and assuming hydrofracture conditions can be achieved. As such, cementation driven by pressure drops is most likely to occur in reverse/thrust faults where the least principal stress is equal to the lithostatic load (Sibson, 2003). For example, several previous studies examining quartz vein systems in thrust settings have inferred a role for large coseismic variations in pore-fluid pressure in quartz precipitation in subduction zones (e.g., Fisher et al., 2019; Saishu et al., 2017; Ujiie et al., 2018; Vrolijk, 1987b), although similar claims have also been made for some normal faults in extensional settings (Parry & Bruhn, 1990). The relatively high pore-fluid pressure gradients achievable in reverse/thrust faults also suggest a potential for particularly fast rates of post-seismic fluid flow where rupture re-establishes hydraulic connectivity with the overlying hydrostatic crust or deeper overpressured fluid reservoirs. The typical low-angle orientation and depressed geothermal gradient of these systems, however, suggests that flow even over kilometer length scales would produce only limited vertical ascent, and therefore limited changes in fluid temperature and pressure when compared to transport through steeper normal or strike-slip faults at higher geothermal gradients. This limitation may be avoided in the case of high-angle reverse faults, where large pore-fluid pressure gradients likely lead to substantial rates of fluid ascent following rupture (Sibson, 1990).

The magnitude and rate of slip may also dictate a variety of factors we infer to control quartz cementation in faults. For example, the potential for kilometer-scale fluid migration may be dependent in part on earthquake magnitude as deformation-related increases in permeability should be preferentially localized within the rupture area, and larger magnitudes imply larger rupture areas (Kanamori & Anderson, 1975). Weatherley and Henley (2013) also showed that the magnitude of pore-fluid pressure variations during earthquakes is proportional to slip magnitude and the length scale of dilational asperities. Little is known, however, regarding the slip rates required to produce large variations in pore-fluid pressure, other than that they must be sufficiently fast to preclude diffusive recovery of pressure from the wallrock. Similarly, the roughness of faults at depth, and associated potential for local dilation, is not easily measured. The magnitude of frictional heating is also directly proportional to slip rates (among other factors). Thus, although the various mechanisms we infer as potential controls on quartz cementation may occur in faults in any setting, it is likely that many of the processes will be enhanced in faults that experience large (meter scale) coseismic displacements during earthquakes. We also recognize that in some locations, smaller faults that are poorly oriented for slip are vein-rich, whereas larger faults that are well oriented for slip are relatively barren of hydrothermal mineralization (e.g., Robert et al., 1995; Sibson & Scott, 1998; Sibson et al., 1988), although this is not a universal observation and vein-rich segments can also occur on well-oriented faults, typically concentrated in bends or step-overs (Cox & Ruming, 2004; Micklethwaite & Cox, 2004; Nguyen et al., 1998). Therefore, although there may be minimum length-scales for effective fluid flow and precipitation, it is not necessarily the largest faults that are most prone to substantial quartz cementation—sufficiently large faults that are also steeply dipping and poorly oriented, enhancing the size of pressure drops, thermal gradient, and potential advective flow, could be where quartz cementation rates are fastest. In our context of cementation within interseismic timescales, we also note that fault segments with minor cements may lack substantial vein systems because rapid healing down dip prevented further fluid flow and cementation.

Finally, interseismic fault healing implies that fault-localized damage heals faster than it is produced by time-averaged slip. As such, regional strain rates may also dictate the potential for quartz cementation to affect fault healing and the seismic cycle. In intraplate faults, for example, relatively low strain rates lead to recurrence intervals that may be several orders of magnitude longer than those typical of plate-boundary faults (Williams, Davis, & Goodwin, 2019). We speculate that some mechanisms leading to fault-localized quartz precipitation, particularly post-seismic fluid migration, may be more effective in facilitating fault healing in faults with longer recurrence intervals simply because the rate of damage production in these systems is slower. We also realize, however, that fluid reservoirs may be smaller in relatively stable interplate regions devoid of tectonically-driven, prograde metamorphism. There is therefore a trade-off between recurrence time and availability of supersaturated fluid, and lack of fluid production may not support the potential for more quartz precipitation that longer time allows. Also note that in systems where earthquake swarms are driven by fluid injection rather than tectonic loading, post-seismic fluid pressure gradients may dissipate quickly following individual swarms, and the length of the interseismic period is then controlled by recovery of fluid overpressure (Cox, 2016). In these settings, the tectonic loading rate has little effect on the potential for cementation, while the effect of fluid production rates may be more important.

3.2. Implications for the Seismic Cycle

Many of the mechanisms we examined for facilitating rapid quartz cementation are difficult to reconcile with sealing of μm-cm wide spaces typical of dilational fault damage zones over interseismic timescales. Those that are on some level reconcilable tend to require specific and extreme circumstances, which may not be consistent with the physical realities of fluid flow, mass transport, and pore-fluid pressure changes in the crust. For example, our calculations show that fluid migration involving multi-kilometer vertical transport may produce quartz precipitation rates capable of sealing damage zone fractures over decadal or shorter time scales, but only at depths where temperatures exceed ∼300°C. We recognize that highly dilatant faults are cemented rapidly in epithermal systems at temperatures <300°C, but shallow fluid boiling is generally required to explain these deposits (e.g., Micklethwaite, 2009; Moncada et al., 2012; Rowland & Simmons, 2012; Sanchez-Alfaro et al., 2016). Coseismic boiling has also been suggested as a mechanism for cement precipitation at greater depths/temperatures (e.g., Weatherley & Henley, 2013), but the establishment of vapor pressure in rapidly dilating fractures likely limits the volume of fluid that is vaporized, resulting in only negligible quartz precipitation and sealing (Williams, 2019). Moreover, cementation of anything more than sub-μm thick increments during advection near the base of the seismogenic crust requires substantial volumes of fluid derived from, and transported through, the ductile lower crust,

where estimated fluid flow rates are typically slow relative to interseismic time scales. These limitations may be alleviated in part by locally increased permeability and fluid flow rates within shear zones during cavitation creep (Fusseis et al., 2009; Menegon et al., 2015) or fluid-driven microcracking (Cox, 2016; Zhang et al., 1994). The temporal and spatial scales of such flow could be a fruitful avenue for future work, as the presence of fault-hosted hydrothermal ore deposits formed at temperatures greater than 300°C requires a mechanism of high flux fluid flow between faults and reservoirs at and below the base of the seismogenic zone (Cox, 1995; Cox et al., 1991; Goldfarb et al., 1991; Sibson & Scott, 1998).

Increased rates of quartz precipitation are also expected in response to large coseismic decreases in pore-fluid pressure, but the extent to which these decreases actually occur in response to earthquakes in the crust is still debatable, as is their spatial scale. Moreover, even if fluid pressure drops as large as a few 100 MPa are assumed, mass balance constraints indicate that only negligible volumes of cement will form in response (i.e., the fracture volumes remain almost entirely unsealed). This process could be sufficient to heal 10–100 μm wide, fault-related cracks in weeks to months, when accompanied by simultaneous fluid advection, as argued by (Ujiie et al., 2018), but it is less likely to heal damage caused by moderate-to-large magnitude earthquakes given the larger mass balance requirements for fluid and silica volumes supplied by fluid advection. Many of the other mechanisms discussed above (i.e., frictional heating; pressure solution; fluid and surface chemistry effects) are much more difficult to constrain in terms of the rate and amount of associated quartz cementation, and represent a fundamental gap in our quantitative understanding of fault healing/sealing associated with quartz cementation. We note, however, that frictional heating and pressure solution are local processes that likely occur preferentially in the immediate vicinity of an earthquake's principal slip surface. As such, these processes may exert a significant influence on overall fault mechanics even if mass balance is limited and the absolute volume of associated cementation is relatively small. Moreover, frictional melting can also locally lead to near-instantaneous cohesive strength recovery as the melt freezes (Hayward & Cox, 2017; Mitchell et al., 2016).

From the above discussion we conclude that the mechanisms we have explored, given current kinetic constraints, cannot explain cementation and sealing of mesoscale fracture networks, even incrementally, over interseismic timescales. Precipitation of mesoscale vein networks, however, may represent a high fluid flux end-member of fault cementation and healing/sealing. For the other end-member of low porosity, low fluid flux, diffusion-dominated systems, recovery of cohesive strength due to cementation has been shown to be possible on 100-year (or faster) timescales in experiments (e.g., Kanagawa et al., 2000; Tenthorey & Cox, 2006) and numerical models (e.g., Hooker & Fisher, 2021 using kinetic-rate parameters from Lander et al., 2008). In such systems, which may be typical of cataclasites or other low-permeability materials localized along fault interfaces, thin (nm-μm) fractures and/or dilational sites could be healed/sealed within days to years. These limited volumes of cement may form within mass balance limitations that restrict formation of larger veins, and although relatively small may significantly impact mechanical and hydrological properties. For example, it may be possible that within fault zones, slip occurs selectively on partially open fractures, after some other fractures have healed completely. This highlights the contrasting permeability regimes and mechanisms of cementation within fault zones, and the possibility of spatially heterogeneous healing and slip. The existence and characteristics of these advective and diffusive end-members remain speculative, but at the first order indicate that high flux scenarios, although more important for voluminous hydrothermal mineralization, may be of subsidiary importance to local, diffusive mass transport in low fluid-flux faults when discussing the mechanical implications of quartz cements in the seismic cycle. We recognize, however, that much of the above discussion focuses on isolated and specific slip-related processes that may lead to quartz cementation and fault healing. These processes are discussed in isolation for clarity and ease of quantification, along with process-specific limitations of the available empirical and theoretical data. It is likely, however, that multiple drivers of quartz precipitation will be active following any moderate to large earthquake event in the crust. As such, we emphasize that many of the discussed mechanisms suffer from fundamental mass balance or other limitations, but we remain open to the possibility of emergent mechanisms of rapid and extensive quartz cementation arising from their interaction.

It is important to recognize that a preponderance of studies have documented fault-localized, cross-cutting vein systems in addition to microstructural evidence of repeated (re)opening and (re)cementation in individual fractures with μm to cm-scale, and frequently larger, opening increments (e.g., Figures 3c and 3d; Boullier & Robert, 1992; Cox, 1987, 1995; Fagereng et al., 2011; Kolb et al., 2004; Laubach et al., 2014; Nguyen et al., 1998; Saishu et al., 2017; Sibson, 1996; Ujiie et al., 2018). Veins in exhumed fault systems also typically

record crystal microstructures indicating that cementation and sealing occurred rapidly relative to the rates of fracture opening and/or collapse (Bons et al., 2012). Although these observations can only strictly be interpreted to record intermittent fracture opening and quartz cementation through time, or temporal variations in fluid chemistry or quartz solubility (Okamoto & Sekine, 2011; Saishu et al., 2014), a link between those processes and recurrent fault slip is certainly permissible, if not probable, particularly where crack-seal structures are observed (Ramsay, 1980). It is at least conceivable, however, that individual crack-seal increments could record more than one interseismic period, in which case the apparent discrepancy between quartz cementation rates and typical interseismic timescales may be reduced. Regardless, the rock record of hydrothermal vein systems seems unambiguous in its support of a seismic cycle influenced by quartz cementation and healing at a wide range of spatial scales (including mesoscale fracture networks in fault damage zones), particularly at hypocentral depths at the base of the brittle crust. When combined with the constraints outlined in this review, we may speculate that the rock record is selective and skewed, and increased preservation potential of extensively cemented, vein-rich faults means that they are over-represented and actually more rare than the geological data imply. They could then represent special conditions of silica kinetics that are rarely achieved. Or alternatively, a lack of understanding and empirical constraints on processes of silica precipitation may mean that we are missing critical components of fault healing mechanisms required to explain the rock record. In either case, a more complete understanding of fault mechanics depends on determining whether cements heal/seal fault rocks over time scales of a few weeks or many decades and whether relatively fast interseismic healing is limited to sub-μm scale deposits along fault interfaces or also cements larger fractures in the surrounding damage zones. It is also unclear whether the cementation that occurs happens immediately following rupture or later in the interseismic period, whether it is discontinuous or can cover large areas, and how fractures at different stages in the healing process interact. The answer to these questions may aid in the development of more mechanistic models describing seismic hazards, where temporal variations in fault strength are paramount to estimating the probability of impending rupture. In this way, our current lack of understanding regarding the mechanisms and rates of quartz cementation in fault zones is of significant societal and scientific importance.

4. Recommendations for Future Research

To address the questions posed above, we end with several recommendations for future research in this area that may be fruitful in increasing our understanding of the mechanisms and rates of quartz cementation in fault zones:

1. *Hydrothermal Experiments.* Hydrothermal quartz growth experiments are uniquely situated to elucidate the controls on quartz precipitation kinetics. These experiments, although once common, have arguably fallen out of favor with geoscientists in the last few decades, in part due to difficulties associated with growing appreciable volumes of quartz under realistic temperatures over laboratory time scales. Many previous experiments, however, were focused on understanding isotopic fractionation or the effect of various growth substrates on overall precipitation habit and rates (Lander et al., 2008; Pollington et al., 2016). We contend that experiments focused on understanding the potential for quartz-cement-related healing need not grow large volumes of cements to be fruitful. Rather, these experiments need only achieve a minimum growth rate resolution as to assess the potential for fracture sealing over interseismic time scales. For example, sealing a 100 μm aperture fracture over 10 years requires a growth rate of 5 μm/yr (assuming growth inward from both fracture walls). This rate implies quartz accumulations of ∼1 μm normal to the growth surface over a 2 month experiment, which are easily resolvable via modern electron microscopy. In this way, when minimum growth-rate resolutions are known, experiments yielding unresolvable volumes of quartz still yield useful information regarding the potential for interseismic cementation over a specific time scales under the imposed experimental conditions. Previous work has already shown that such experiments are useful for understanding the effects of mineral surface chemistry and the presence of amorphous silica (e.g., Williams, Farver, et al., 2015) in addition to pressure solution (e.g., Tenthorey & Cox, 2006; Tenthorey et al., 2003) and crystallographic effects (e.g., Lander et al., 2008). We argue that additional work in this area is similarly likely to yield the critical, empirical, kinetic constraints necessary to better interpret the rock record of quartz-cementation in exhumed faults.
2. *Direct Constraints on Quartz Precipitation Rates in Nature.* The rock record of exhumed fault zones is ultimately the only source of directly assessing the rates of fault-localized quartz cementation. Recent advances in geochronology have permitted reconstruction of the rates and timescales of cementation/mineralization in

faults other mineral systems (i.e., calcite, hematite, clays; Ault, 2020; Ault et al., 2016; Mottram et al., 2020; Roberts et al., 2020; Scheiber et al., 2019; Uysal et al., 2011; Williams, Mozley, et al., 2019). Unfortunately, quartz is generally not amenable to currently available geochronological techniques. We suggest, however, that there are still several avenues along which quartz-precipitation rates may be obtained in the rock record. First, although cements precipitated directly as quartz are unlikely to be dateable, this is not true of other metastable silica phases, even following recrystallization to a more stable polymorphs. Recent work, for example, has illustrated the utility of U-Pb dating of silica veins to reconstruct fault-zone fluid flow histories in the Eastern California Shear Zone (Nuriel et al., 2019). Moreover, even in situations where quartz is not dateable, crack-seal growth increments in fractures may be lined by phyllosilicate or other inclusion bands (e.g., Ujiie et al., 2018), which may be amenable to geochronology depending on their age, mineralogy, and origin with respect to fault activity. Finally, previous work has been successful in providing constraints on quartz precipitation rates in fractures in sedimentary basins by combining paleothermometeric analysis of quartz veins with well-defined thermochronologic data of the surrounding rocks (Becker et al., 2010; Fall et al., 2015; Hooker et al., 2015). Given that crystalline rocks are generally more amenable than sedimentary units to thermochronologic approaches, we contend that similar strategies may provide insight into quartz precipitation rates in more deeply exhumed systems. Some more recent work has also demonstrated the utility of Li isotope diffusion studies in estimating rates of crystal growth in fractures (Taetz et al., 2018).

3. *Fluid Flow and Mass Transport Deep in Seismogenic Faults.* Geochemical examination of fault zone cements have proven useful for quantifying the source of mineralizing fluids, which when examined within a robust structural and tectonic framework allows reconstruction of fault permeability structures and mechanisms of mass transport (e.g., Beaudoin & Pitre, 2005; Bohlke & Kistler, 1986; Boles et al., 2015; Nesbitt et al., 1989; Smeraglia et al., 2016; Stenvall et al., 2020; Taetz et al., 2018; Williams, Beard, et al., 2019; Williams, Goodwin, et al., 2015). Critically, however, many of the recent advances in this area of research have been focused on exposures exhumed from the uppermost few kilometers of the seismogenic crust. We suggest that the application of similar studies to quartz cementation in fault rocks exhumed from hypocentral depths (10–15 km or greater) near the brittle-ductile transition may yield important insights into the mechanisms driving quartz cementation. Although not direct constraints of cementation rates, knowing the driving mechanisms of cementation is critical to constrain models and design experiments. For example, the documentation of mineralizing fluids equilibrated external to the site of precipitation must imply some role for fluid advection. Evidence of fluids equilibrated with the local wall rock could either imply external fluids that have a rock-buffered chemistry, or locally-sourced fluids. The latter implies a diffusive mass-transport regime, which may be most consistent with coseismic variations in pore-fluid pressure, pressure solution, or growth driven by frictional heating. Analytical limitations and a lack of systematic understanding of many isotopic systems have largely limited studies of quartz growth to oxygen isotope analysis. Recent work in other mineral systems (i.e., calcite, hematite, and clays), and expanded use of other isotopic systems (i.e., Li, Si, Sr, Pb, Nd, etc.) and rare-earth element analysis, have shown increased ability to differentiate fluid sources and mass transport pathways (e.g., Eichhubl & Boles, 2000; Taetz et al., 2018; Williams, Beard, et al., 2019). Although these elements are found in limited concentration in quartz (with the exception of Si), it is likely that modern mass spectrometry approaches will allow their quantification, and that these new approaches expand the potential for delineating fluid and mass transport pathways during quartz cementation deep in the seismogenic crust, including spatiotemporal variation in flow and cementation within single fault zones.
4. *Interdisciplinary Research.* All of the above recommendations require a renewed focus on holistic analyses of fault zones and fault processes, which can only be accomplished via truly interdisciplinary research. Examples of interdisciplinary studies that could be attempted with existing technology include: (a) combining detailed field and geochemical studies of vein systems with numerical models that track fluid and vein chemistry, and can therefore directly compare models with nature; (b) hydrothermal experiments that constrain precipitation rates being coupled to field observations that constrain boundary conditions and calibrate numerical models that aid extrapolation across temporal and spatial scales; and (c) deformation experiments that quantify the role of cements, of different geometry and microstructure, in determining the strength of faults. We argue that these and similar interdisciplinary approaches, while here designed to better constrain fluid-fault interactions, invariably produce additional, emergent discoveries that cannot be anticipated. As such, increased efforts in this area are required to improve our understanding of quartz cementation and fault healing, but will likely result in additional research endeavors far beyond the scope of those discussed here.

5. Conclusions

We critically review and present both quantitative and qualitative constraints on the rates of quartz precipitation and associated healing in faults and fractures in the brittle crust. We find that many of the mechanisms we examined for facilitating rapid quartz cementation (i.e., over the 100-year time scales typical of an interseismic period) and healing, although commonly invoked, are difficult to reconcile with the timescales of the seismic cycle and spatial scale of fault-related vein systems exhumed from conditions where $200°C \leq T \leq 350°C$. Upward fluid discharge along faults following rupture, for example, may facilitate fracture cementation and sealing over interseismic timescales, but can only fill μm-cm aperture fractures if the vertical component of fluid transport is multi-kilometer in scale. The rates of likely fluid transport near the base of the seismogenic crust, however, imply significant time lags between rupture and the onset of cementation at a particular depth. Another popular mechanism argued to facilitate cementation in faults—coseismic dilational deformation and associated fluid decompression—suffers from significant mass balance limitations. These limitations indicate that no magnitude of coseismic pressure decrease can be expected to drive sealing of fractures in the absence of large-scale fluid advection. Other mechanisms that may facilitate local quartz supersaturation and fault cementation, such as frictional heating and pressure solution, may provide more realistic mechanisms of fault healing local to the principal slip surface(s), but these cannot explain the abundance of cement commonly observed in veins in the surrounding damage zones. Collectively, these calculations contrast starkly with rock-record observations, which suggest a seismic cycle linked to permeability variations that allow episodic fluid flow and vein precipitation in fault and damage zone vein networks.

The limitations to the kinetics and mass balance of silica precipitation that we have presented here lead us to emphasize two end-member regimes. On the one hand, the mechanisms we have explored, given current kinetic constraints, cannot explain mesoscale fault and fracture vein networks developing, even incrementally, on interseismic timescales. Two interpretations can explain this contradiction. The first is that extensively quartz-cemented, vein-rich faults are over-represented in the rock record and actually form less frequently than the geological observations imply. The second is that we are missing critical components of the cementation mechanisms required to explain the rock record, because we lack understanding and empirical constraints on processes of silica precipitation. It may also be that these dilatant, potentially high fluid flux fracture systems do not typically close over interseismic periods, but are instead at least partially open and maybe, episodically, isolated from fluid reservoirs. On the other hand, the mechanisms we explored appear capable, isolated or in combination, to cement thin (nm-μm) fractures and/or dilational sites (e.g., those in cataclasites lining slip surface), which could allow mechanical and hydrological sealing of principal slip surfaces within days, weeks, or years after a rupture. This does not explain the vein networks commonly developed in fault damage zones, but allows the involvement of quartz cements in fault healing, and highlights the contrasting permeability regimes and mechanisms of cementation within fault zones. These end-members may imply, perhaps surprisingly, that high-flux faults dominated by advective transport are more difficult to heal quickly than low-flux faults dominated by diffusive transport, because of kinetic and mass balance challenges in healing the larger fracture volumes that facilitate high-flux flow. The presence of extensive vein systems in the rock record, however, implies that sealing during high fluid flux is achieved at least under some conditions, potentially between discrete slip events. The existence and characteristics of these end-members, and their relative importance in hydrothermal precipitation and fault mechanics, remain speculative. We hypothesize that high flux scenarios, although more important for voluminous hydrothermal mineralization, may be of subsidiary importance to local, diffusive mass transport in low fluid-flux faults when discussing the mechanical implications of quartz cements. A renewed emphasis on research examining the controls on the rates of quartz cementation in fault zones will, however, be integral to developing a more complete understanding of the mechanisms and timescales of strength recovery following earthquake rupture.

Glossary

Cementation Precipitation of minerals or other solid phases from fluids within the interstitial space of a rock mass. Cementation typically acts to decrease permeability whilst simultaneously increase mechanical strength.

Seismic/Earthquake Cycle The time period during which faults accumulate elastic strain due to plate motion, and/or frictional resistance decreases as fluid pressure builds up, and accumulated strain is rapidly released during earthquakes. Here, we consider a single seismic cycle to encompass inter-seismic, co-seismic, and post-seismic periods between two successive earthquakes on the same fault segment.

Coseismic	The period of time during earthquake rupture.
Post-seismic	A time period of transient deformation following an earthquake rupture and before the onset of steady interseismic elastic strain accumulation.
Interseismic	The period of time between successive earthquake ruptures. Also referred to as "repeat time" or "recurrence interval." The interseismic period includes the post-seismic period by definition. The interseismic period is typically a few 100 years or less in active, plate-boundary faults.
Seismogenic Crust/Zone	The depth range in the crust where earthquakes typically nucleate. The base of the seismogenic crust/zone in continents is generally thought to coincide with the onset of crystal-plastic/ductile behavior in quartz at temperatures of about 300°C–350°C. This is, however, not a sharp transition and an intermediate regime involving frictional-viscous behavior and/or frictional creep can separate the dominantly frictional and crystal-plastic regimes.
Healing	The phenomenon of time-dependent increases in the strength of faults and fault rocks following slip. This process likely encompasses a variety of physical and chemical mechanisms that differ at varying depths in the crust.
Lithostatic Pressure	Pressure exerted on a rock mass by the weight of the overlying material. Sometimes referred to as "overburden" pressure. Lithostatic pressure is commonly considered to be an upper bound on pore-fluid pressure in the crust, as pore-fluid pressures in excess of the least compressive stress (which is less than or equal to the lithostatic pressure) likely lead to hydrofracturing and pressure release. The lithostatic gradient as a function of depth varies with rock type, but a value of ∼26.2 MPa/km is considered typical.
Hydrostatic Pressure	Pressure exerted at any point in an interconnected water column that results from the weight of the overlying water. Hydrostatic conditions are typically considered to be a lower bound on pore-fluid pressure in the crust, although exceptions exist, for example, where sub-hydrostatic conditions are created through fluid-consumption by metamorphic reactions or after burial of relatively dry, highly impermeable rocks. The hydrostatic gradient as a function of depth is 9.8 MPa/km.
Overpressure	A condition where pore-fluid pressures at a point in the crust exceed hydrostatic values.
Equilibrium Solubility	The concentration of a mineral phase in solution at equilibrium conditions, typically controlled by in situ temperature and pressure. In this paper, equilibrium solubility may be considered synonymous with "pre-failure" or "pre-slip" solubility. Fluids that have achieved equilibrium solubility with respect to a particular dissolved mineral phase are considered to be "saturated."
Supersaturation	A condition where the actual concentration of a dissolved mineral in solution exceeds the equilibrium solubility, leading to precipitation of the solid form. For the purposes of this paper, supersaturation occurs when the concentration of silica in solution at some time and place of interest ($CSiO_2$) exceeds the equilibrium solubility ($CSiO_{2-eq}$) (i.e., supersaturation is achieved when $\Omega = CSiO_2/CSiO_{2-eq} > 1$).
Amorphous or Metastable Phases	Non- or poorly-crystalline phases that are typically unstable and therefore highly reactive. For silica, these phases typically have lower activation energies for precipitation than quartz, and thus can precipitate at faster rates under equal conditions.
Kinetics	A description of the rates of chemical reactions and their controls. Often strongly dependent on temperature.

Pressure Solution	A process by which solubility of a mineral phase is enhanced at high-stress, grain-to-grain contacts leading to localized dissolution. Reprecipitation may (or may not) then occur at sites of relatively lower stress.
Dissolution-Precipitation Creep	The collective process of dissolution by pressure solution, transport in a stationary or moving fluid phase, and re-precipitation at a lower-stress site.

Data Availability Statement

All MATLAB code and associated descriptions and input data are available with an Open Science Foundation repository at https://doi.org/10.17605/OSF.IO/CT63A.

Acknowledgments
The authors thank Rob Lander for helpful discussions related to discrepancies between natural and experimentally constrained quartz growth rates, and specifically credit him with the idea that the difference may stem from non-linearities in rate at near-equilibrium supersaturations. R. T. Williams would like to thank John Farver and Charles Onasch for introducing him to this field of research and for providing a wayward young person with the opportunity to take a different path. This material is based upon work supported by the National Science Foundation under Grant No. EAR-1951985. A. Fagereng recalls with appreciation many quartz-related discussions with Rick Sibson, and acknowledges the European Research Council (ERC) for funding under the European Union's Horizon 2020 research and innovation program (grant agreement no 715836 "MICA"). The authors thank Stephen Cox and an anonymous reviewer for constructive reviews that improved the quality of this work. Descriptions of methodology and complete MATLAB codes used for this work can be found in Supporting Information S1.

References

Ague, J. (1995). Deep crustal growth of quartz, kyanite and garnet into large-aperture, fluid-filled fractures, north-eastern Connecticut, USA. *Journal of Metamorphic Geology*, *13*(2), 299–314. https://doi.org/10.1111/j.1525-1314.1995.tb00220.x

Amagai, T., Okamoto, A., Niibe, T., Hirano, N., Motomiya, K., & Tsuchiya, N. (2019). Silica nanoparticles produced by explosive flash vaporization during earthquakes. *Scientific Reports*, *9*(1), 1–9. https://doi.org/10.1038/s41598-019-46320-7

Ault, A. K. (2020). Hematite fault rock thermochronometry and textures inform fault zone processes. *Journal of Structural Geology*, *133*, 104002. https://doi.org/10.1016/j.jsg.2020.104002

Ault, A. K., Frenzel, M., Reiners, P. W., Woodcock, N. H., & Thomson, S. N. (2016). Record of paleofluid circulation in faults revealed by hematite (U-Th)/He and apatite fission-track dating: An example from Gower Peninsula fault fissures, Wales. *Lithosphere*, *8*(4), 379–385. https://doi.org/10.1130/l522.1

Beaudoin, G., & Pitre, D. (2005). Stable isotope geochemistry of the Archean Val-d'Or (Canada) orogenic gold vein field. *Mineralium Deposita*, *40*(1), 59–75. https://doi.org/10.1007/s00126-005-0474-z

Becker, S., Eichhubl, P., Laubach, S., Reed, R., Lander, R., & Bodnar, R. (2010). A 48 my history of fracture opening, temperature, and fluid pressure: Cretaceous Travis Peak Formation, East Texas basin. *Bulletin*, *122*(7–8), 1081–1093. https://doi.org/10.1130/b30067.1

Beeler, N., & Tullis, T. (1996). Self-healing slip pulses in dynamic rupture models due to velocity-dependent strength. *Bulletin of the Seismological Society of America*, *86*(4), 1130–1148.

Bestmann, M., Pennacchioni, G., Mostefaoui, S., Göken, M., & de Wall, H. (2016). Instantaneous healing of micro-fractures during coseismic slip: Evidence from microstructure and Ti in quartz geochemistry within an exhumed pseudotachylyte-bearing fault in tonalite. *Lithos*, *254*, 84–93. https://doi.org/10.1016/j.lithos.2016.03.011

Bettermann, P., & Liebau, F. (1975). The transformation of amorphous silica to crystalline silica under hydrothermal conditions. *Contributions to Mineralogy and Petrology*, *53*(1), 25–36. https://doi.org/10.1007/bf00402452

Blenkinsop, T. (2008). Relationships between faults, extension fractures and veins, and stress. *Journal of Structural Geology*, *30*(5), 622–632. https://doi.org/10.1016/j.jsg.2008.01.008

Bohlke, J., & Kistler, R. (1986). Rb-Sr, K-Ar, and stable isotope evidence for the ages and sources of fluid components in the northern Sierra Nevada foothills metamorphic belt, California. *Economic Geology*, *81*, 296–322.

Boles, A., van der Pluijm, B., Mulch, A., Mutlu, H., Uysal, I. T., & Warr, L. N. (2015). Hydrogen and $^{40}Ar/^{39}Ar$ isotope evidence for multiple and protracted paleofluid flow events within the long-lived North a Natolian Keirogen (Turkey). *Geochemistry, Geophysics, Geosystems*, *16*(6), 1975–1987. https://doi.org/10.1002/2015gc005810

Bons, P. D., Elburg, M. A., & Gomez-Rivas, E. (2012). A review of the formation of tectonic veins and their microstructures. *Journal of Structural Geology*, *43*, 33–62. https://doi.org/10.1016/j.jsg.2012.07.005

Borhara, K., & Onasch, C. M. (2020). Evidence for silica gel and its role in faulting in the Tuscarora Sandstone. *Journal of Structural Geology*, *139*(104), 140. https://doi.org/10.1016/j.jsg.2020.104140

Bos, B., & Spiers, C. (2000). Effect of phyllosilicates on fluid-assisted healing of gouge-bearing faults. *Earth and Planetary Science Letters*, *184*(1), 199–210. https://doi.org/10.1016/s0012-821x(00)00304-6

Boullier, A.-M., & Robert, F. (1992). Palaeoseismic events recorded in Archaean gold-quartz vein networks, Val d'Or, Abitibi, Quebec, Canada. *Journal of Structural Geology*, *14*(2), 161–179. https://doi.org/10.1016/0191-8141(92)90054-z

Brantley, S. L., Evans, B., Hickman, S. H., & Crerar, D. A. (1990). Healing of microcracks in quartz: Implications for fluid flow. *Geology*, *18*(2), 136–139. https://doi.org/10.1130/0091-7613(1990)018

Brantut, N. (2020). Dilatancy-induced fluid pressure drop during dynamic rupture: Direct experimental evidence and consequences for earthquake dynamics. *Earth and Planetary Science Letters*, *538*(116), 179. https://doi.org/10.1016/j.epsl.2020.116179

Braun, J., Munroe, S. M., & Cox, S. (2003). Transient fluid flow in and around a fault. *Geofluids*, *3*(2), 81–87. https://doi.org/10.1046/j.1468-8123.2003.00051.x

Breeding, C. M., & Ague, J. J. (2002). Slab-derived fluids and quartz-vein formation in an accretionary prism, Otago Schist, New Zealand. *Geology*, *30*(6), 499–502. https://doi.org/10.1130/0091-7613(2002)030<0499:sdfaqv>2.0.co;2

Burch, T., Nagy, K., & Lasaga, A. (1993). Free energy dependence of albite dissolution kinetics at 80°C and pH 8.8. *Chemical Geology*, *105*(1–3), 137–162. https://doi.org/10.1016/0009-2541(93)90123-z

Caine, J. S., Evans, J. P., & Forster, C. B. (1996). Fault zone architecture and permeability structure. *Geology*, *24*(11). https://doi.org/10.1130/0091-7613(1996)024<1025

Callahan, O. A., Eichhubl, P., & Davatzes, N. C. (2020). Mineral precipitation as a mechanism of fault core growth. *Journal of Structural Geology*, *140*, 104156. https://doi.org/10.1016/j.jsg.2020.104156

Cardwell, R., Chinn, D., Moore, G., & Turcotte, D. (1978). Frictional heating on a fault zone with finite thickness. *Geophysical Journal International*, *52*(3), 525–530. https://doi.org/10.1111/j.1365-246x.1978.tb04247.x

Carpenter, B., Marone, C., & Saffer, D. (2011). Weakness of the San Andreas Fault revealed by samples from the active fault zone. *Nature Geoscience*, *4*(4), 251–254. https://doi.org/10.1038/ngeo1089

Cook, J. E., Dunne, W. M., & Onasch, C. M. (2006). Development of a dilatant damage zone along a thrust relay in a low-porosity quartz arenite. *Journal of Structural Geology*, *28*(5), 776–792. https://doi.org/10.1016/j.jsg.2006.02.007

Cox, S. (2010). The application of failure mode diagrams for exploring the roles of fluid pressure and stress states in controlling styles of fracture-controlled permeability enhancement in faults and shear zones. *Geofluids*, *10*(1–2), 217–233. https://doi.org/10.1111/j.1468-8123.2010.00281.x

Cox, S., & Ruming, K. (2004). The St Ives mesothermal gold system, Western Australia—A case of golden aftershocks? *Journal of Structural Geology*, *26*(6), 1109–1125. https://doi.org/10.1016/j.jsg.2003.11.025

Cox, S., Wall, V., Etheridge, M., & Potter, T. (1991). Deformational and metamorphic processes in the formation of mesothermal vein-hosted gold deposits — Examples from the Lachlan Fold Belt in central Victoria, Australia. *Ore Geology Reviews*, *6*(5), 391–423. https://doi.org/10.1016/0169-1368(91)90038-9

Cox, S. F. (1987). Antitaxial crack-seal vein microstructures and their relationship to displacement paths. *Journal of Structural Geology*, *9*(7), 779–787. https://doi.org/10.1016/0191-8141(87)90079-4

Cox, S. F. (2005). Coupling between deformation, fluid pressures, and fluid flow in ore-producing hydrothermal systems at depth in the crust. *Economic Geology*, *100*, 39–75. https://doi.org/10.5382/av100.04

Cox, S. F. (1995). Faulting processes at high fluid pressures: An example of fault valve behavior from the Wattle Gully Fault, Victoria, Australia. *Journal of Geophysical Research*, *100*(B7), 12841–12859. https://doi.org/10.1029/95JB00915

Cox, S. F. (2016). Injection-driven swarm seismicity and permeability enhancement: Implications for the dynamics of hydrothermal ore systems in high fluid-flux, overpressured faulting regimes—An invited paper. *Economic Geology*, *111*(3), 559–587. https://doi.org/10.2113/econgeo.111.3.559

Cox, S. F., & Munroe, S. M. (2016). Breccia formation by particle fluidization in fault zones: Implications for transitory, rupture-controlled fluid flow regimes in hydrothermal systems. *American Journal of Science*, *316*(3), 241–278. https://doi.org/10.2475/03.2016.02

Curewitz, D., & Karson, J. A. (1999). Ultracataclasis, sintering, and frictional melting in pseudotachylytes from East Greenland. *Journal of Structural Geology*, *21*(12), 1693–1713. https://doi.org/10.1016/s0191-8141(99)00119-4

de Ronde, C. E. J., Sibson, R. H., Bray, C. J., & Faure, K. (2001). Fluid chemistry of veining associated with an ancient microearthquake swarm, Benmore Dam, New Zealand. *The Geological Society of America Bulletin*, *113*(8), 1010–1024. https://doi.org/10.1130/0016-7606(2001)113<1010:fcovaw>2.0.co;2

Dieterich, J. H. (1972). Time-dependent friction in rocks. *Journal of Geophysical Research*, *77*(20), 3690–3697. https://doi.org/10.1029/JB077i020p03690

Dolejš, D., & Manning, C. (2010). Thermodynamic model for mineral solubility in aqueous fluids: Theory, calibration and application to model fluid-flow systems. *Geofluids*, *10*(1–2), 20–40. https://doi.org/10.1111/j.1468-8123.2010.00282.x

Dong, G., Morrison, G., & Jaireth, S. (1995). Quartz textures in epithermal veins, Queensland – Classification, origin, and implication. *Economic Geology*, *90*(6), 1841–1856. https://doi.org/10.2113/gsecongeo.90.6.1841

Dove, P., & Rimstidt, J. (1994). Silicon-water interactions. In P. J. Heaney, C. T. Prewitt, & G. V. Gibbs (Eds.), *Silic-physical behaviour, geochemistry and materials applications* (Vol. 29, p. 258). *Review in Mineralogy*. Mineralogical Society of America.

Dove, P. M. (1994). The dissolution kinetics of quartz in sodium chloride solutions at 25 to 300. *American Journal of Science*, *294*(6), 665–712. https://doi.org/10.2475/ajs.294.6.665

Dove, P. M., & Crerar, D. A. (1990). Kinetics of quartz dissolution in electrolyte solutions using a hydrothermal mixed flow reactor. *Geochimica et Cosmochimica Acta*, *54*(4), 955–969. https://doi.org/10.1016/0009-2541(90)90244-2

Durney, D. (1972). Solution-transfer, an important geological deformation mechanism. *Nature*, *235*(5337), 315–317. https://doi.org/10.1038/235315a0

Eichhubl, P., & Boles, J. R. (2000). Focused fluid flow along faults in the Monterey Formation, coastal California. *The Geological Society of America Bulletin*, *112*(11), 1667–1679. https://doi.org/10.1130/0016-7606(2000)112<1667:fffafi>2.0.co;2

Eichhubl, P., Davatzes, N. C., & Becker, S. P. (2009). Structural and diagenetic control of fluid migration and cementation along the Moab fault, Utah. *AAPG Bulletin*, *93*(5), 653–681. https://doi.org/10.1306/02180908080

Elias, B. P., & Hajash, A., Jr. (1992). Changes in quartz solubility and porosity due to effective stress: An experimental investigation of pressure solution. *Geology*, *20*(5), 451–454. https://doi.org/10.1130/0091-7613(1992)020<0451:ciqsap>2.3.co;2

Evans, J. P., Forster, C. B., & Goddard, J. V. (1997). Permeability of fault-related rocks, and implications for hydraulic structure of fault zones. *Journal of Structural Geology*, *19*(11), 1393–1404. https://doi.org/10.1016/s0191-8141(97)00057-6

Evans, K. F., Genter, A., & Sausse, J. (2005). Permeability creation and damage due to massive fluid injections into granite at 3.5 km at Soultz: 1. Borehole observations. *Journal of Geophysical Research*, *110*(B4). https://doi.org/10.1029/2004jb003168

Faber, C., Rowe, C. D., Miller, J. A., Fagereng, Å., & Neethling, J. H. (2014). Silica gel in a fault slip surface: Field evidence for palaeo-earthquakes? *Journal of Structural Geology*, *69*, 108–121. https://doi.org/10.1016/j.jsg.2014.09.021

Fagereng, Å., Diener, J. F., Meneghini, F., Harris, C., & Kvadsheim, A. (2018). Quartz vein formation by local dehydration embrittlement along the deep, tremorgenic subduction thrust interface. *Geology*, *46*(1), 67–70. https://doi.org/10.1130/g39649.1

Fagereng, Å., Remitti, F., & Sibson, R. H. (2011). Incrementally developed slickenfibers—Geological record of repeating low stress-drop seismic events? *Tectonophysics*, *510*(3–4), 381–386. https://doi.org/10.1016/j.tecto.2011.08.015

Faleiros, A. M., Campanha, G. A. d. C., Faleiros, F. M., & Bello, R. M. d. S. (2014). Fluid regimes, fault-valve behavior and formation of gold-quartz veins—The Morro do Ouro Mine, Ribeira Belt, Brazil. *Ore Geology Reviews*, *56*, 442–456. https://doi.org/10.1016/j.oregeorev.2013.05.002

Fall, A., Eichhubl, P., Bodnar, R. J., Laubach, S. E., & Davis, J. S. (2015). Natural hydraulic fracturing of tight-gas sandstone reservoirs, Piceance Basin, Colorado. *Bulletin*, *127*(1–2), 61–75. https://doi.org/10.1130/b31021.1

Fisher, D., & Byrne, T. (1990). The character and distribution of mineralized fractures in the Kodiak Formation, Alaska: Implications for fluid flow in an underthrust sequence. *Journal of Geophysical Research*, *95*(B6), 9069–9080. https://doi.org/10.1029/jb095ib06p09069

Fisher, D. M., Smye, A. J., Marone, C., van Keken, P., & Yamaguchi, A. (2019). Kinetic models for healing of the subduction interface based on observations of ancient accretionary complexes. *Geochemistry, Geophysics, Geosystems*, *20*(7), 3431–3449. https://doi.org/10.1029/2019gc008256

Fleming, B., & Crerar, D. (1982). Silicic acid ionization and calculation of silica solubility at elevated temperature and pH application to geothermal fluid processing and reinjection. *Geothermics*, *11*(1), 15–29. https://doi.org/10.1016/0375-6505(82)90004-9

Fournier, R., & Potter, R. (1982a). Revised and expanded silica (quartz) geothermometer. *Bulletin Geothermal Resources Council*, *11*(10).

Fournier, R. O., & Potter, R. W. (1982b). An equation correlating the solubility of quartz in water from 25 to 900°C at pressures up to 10,000 bars. *Geochimica et Cosmochimica Acta*, *46*(10), 1969–1973. https://doi.org/10.1016/0016-7037(82)90135-1

Fusseis, F., Regenauer-Lieb, K., Liu, J., Hough, R. M., & De Carlo, F. (2009). Creep cavitation can establish a dynamic granular fluid pump in ductile shear zones. *Nature*, *459*(7249), 974–977. https://doi.org/10.1038/nature08051

Giger, S. B., Cox, S. F., & Tenthorey, E. (2008). Slip localization and fault weakening as a consequence of fault gouge strengthening — Insights from laboratory experiments. *Earth and Planetary Science Letters*, *276*(1), 73–84. https://doi.org/10.1016/j.epsl.2008.09.004

Giger, S. B., Tenthorey, E., Cox, S. F., & Fitz Gerald, J. D. (2007). Permeability evolution in quartz fault gouges under hydrothermal conditions. *Journal of Geophysical Research*, *112*(B7), B07202. https://doi.org/10.1029/2006jb004828

Goldfarb, R. J., Snee, L. W., Miller, L. D., & Newberry, R. J. (1991). Rapid dewatering of the crust deduced from ages of mesothermal gold deposits. *Nature*, *354*(6351), 296–298. https://doi.org/10.1038/354296a0

Goodwin, L. B. (1999). Controls on pseudotachylyte formation during tectonic exhumation in the South Mountains metamorphic core complex, Arizona. *Geological Society, London, Special Publications*, *154*(1), 325–342. https://doi.org/10.1144/gsl.sp.1999.154.01.15

Gosselin, J. M., Audet, P., Estève, C., McLellan, M., Mosher, S. G., & Schaeffer, A. J. (2020). Seismic evidence for megathrust fault-valve behavior during episodic tremor and slip. *Science Advances*, *6*(4), eaay5174. https://doi.org/10.1126/sciadv.aay5174

Gratier, J.-P., Dysthe, D. K., & Renard, F. (2013). The role of pressure solution creep in the ductility of the Earth's upper crust. In *Advances in Geophysics* (Vol. 54, pp. 47–179). Elsevier.

Hayward, K. S., & Cox, S. F. (2017). Melt welding and its role in fault reactivation and localization of fracture damage in seismically active faults. *Journal of Geophysical Research: Solid Earth*, *122*(12), 9689–9713. https://doi.org/10.1002/2017JB014903

Herrington, R. J., & Wilkinson, J. J. (1993). Colloidal gold and silica in mesothermal vein systems. *Geology*, *21*(6), 539–542. https://doi.org/10.1130/0091-7613(1993)021<0539:cgasim>2.3.co;2

Hirono, T., Kaneki, S., Ishikawa, T., Kameda, J., Tonoike, N., Ito, A., & Miyazaki, Y. (2020). Generation of sintered fault rock and its implications for earthquake energetics and fault healing. *Communications Earth & Environment*, *1*(1), 1–8. https://doi.org/10.1038/s43247-020-0004-z

Hooker, J., & Fisher, D. (2021). How cementation and fluid flow influence slip behavior at the subduction interface. *Geology*.

Hooker, J. N., Larson, T. E., Eakin, A., Laubach, S. E., Eichhubl, P., Fall, A., & Marrett, R. (2015). Fracturing and fluid flow in a sub-décollement sandstone; or, a leak in the basement. *Journal of the Geological Society*, *172*(4), 428–442. https://doi.org/10.1144/jgs2014-128

Hosaka, M., & Taki, S. (1981). Hydrothermal growth of quartz crystals in KC1 solution. *Journal of Crystal Growth*, *53*(3), 542–546. https://doi.org/10.1016/0022-0248(81)90137-8

Houseknecht, D. W. (1984). Influence of grain size and temperature on intergranular pressure solution, quartz cementation, and porosity in a quartzose sandstone. *Journal of Sedimentary Research*, *54*(2), 348–361. https://doi.org/10.1306/212F8418-2B24-11D7-8648000102C1865D

Husen, S., & Kissling, E. (2001). Postseismic fluid flow after the large subduction earthquake of Antofagasta, Chile. *Geology*, *29*(9), 847–850. https://doi.org/10.1130/0091-7613(2001)029<0847:pffatl>2.0.co;2

Jiang, J., & Lapusta, N. (2017). Connecting depth limits of interseismic locking, microseismicity, and large earthquakes in models of long-term fault slip. *Journal of Geophysical Research*, *122*(8), 6491–6523. https://doi.org/10.1002/2017jb014030

Kanagawa, K., Cox, S. F., & Zhang, S. (2000). Effects of dissolution-precipitation processes on the strength and mechanical behavior of quartz gouge at high-temperature hydrothermal conditions. *Journal of Geophysical Research*, *105*(B5), 11115–11126. https://doi.org/10.1029/2000jb900038

Kanamori, H., & Allen, C. (1986). Earthquake repeat time and average stress drop. In S. Das, J. Boatwright, & C. H. Scholz (Eds.), Earthquake source mechanics. Geophysical Monograph Series (Vol. 37, pp. 227–235). American Geophysical Union.

Kanamori, H., & Anderson, D. L. (1975). Theoretical basis of some empirical relations in seismology. *Bulletin of the Seismological Society of America*, *65*(5), 1073–1095.

Karner, S. L., & Marone, C. (2000). Effects of loading rate and normal stress on stress drop and stick-slip recurrence interval. *Geophysical Monograph-American Geophysical Union*, *120*, 187–198. https://doi.org/10.1029/gm120p0187

Kirkpatrick, J. D., Dobson, K. J., Mark, D. F., Shipton, Z. K., Brodsky, E. E., & Stuart, F. M. (2012). The depth of pseudotachylyte formation from detailed thermochronology and constraints on coseismic stress drop variability. *Journal of Geophysical Research*, *117*(B6). https://doi.org/10.1029/2011JB008846

Kirkpatrick, J. D., Rowe, C. D., White, J. C., & Brodsky, E. E. (2013). Silica gel formation during fault slip: Evidence from the rock record. *Geology*, *41*(9), 1015–1018. https://doi.org/10.1130/g34483.1

Kolb, J., Rogers, A., Meyer, F. M., & Vennemann, T. W. (2004). Development of fluid conduits in the auriferous shear zones of the Hutti Gold Mine, India: Evidence for spatially and temporally heterogeneous fluid flow. *Tectonophysics*, *378*(1–2), 65–84. https://doi.org/10.1016/j.tecto.2003.10.009

Lachenbruch, A. H. (1986). *Simple models for the estimation and measurement of frictional heating by an earthquake*. US Department of the Interior, Geological Survey.

Lander, R., & Laubach, S. (2015). Insights into rates of fracture growth and sealing from a model for quartz cementation in fractured sandstones. *Bulletin*, *127*(3–4), 516–538. https://doi.org/10.1130/b31092.1

Lander, R. H., Larese, R. E., & Bonnell, L. M. (2008). Toward more accurate quartz cement models: The importance of euhedral versus noneuhedral growth rates. *AAPG Bulletin*, *92*(11), 1537–1563. https://doi.org/10.1306/07160808037

Lasaga, A. C. (1981). Rate laws of chemical reactions. *Reviews in Mineralogy*; (United States), *8*.

Laubach, S. E., Eichhubl, P., Hargrove, P., Ellis, M. A., & Hooker, J. N. (2014). Fault core and damage zone fracture attributes vary along strike owing to interaction of fracture growth, quartz accumulation, and differing sandstone composition. *Journal of Structural Geology*, *68*, 207–226. https://doi.org/10.1016/j.jsg.2014.08.007

Laubach, S. E., Lander, R., Criscenti, L. J., Anovitz, L. M., Urai, J., Pollyea, R., et al. (2019). The role of chemistry in fracture pattern development and opportunities to advance interpretations of geological materials. *Reviews of Geophysics*, *57*(3), 1065–1111. https://doi.org/10.1029/2019rg000671

Lin, A., Tanaka, N., Uda, S., & Satish-Kumar, M. (2003). Repeated coseismic infiltration of meteoric and seawater into deep fault zones: A case study of the Nojima fault zone, Japan. *Chemical Geology*, *202*(1–2), 139–153. https://doi.org/10.1016/j.chemgeo.2003.08.010

Louis, S., Luijendijk, E., Dunkl, I., & Person, M. (2019). Episodic fluid flow in an active fault. *Geology*, *47*(10), 938–942. https://doi.org/10.1130/g46254.1

Manning, C. E. (1994). The solubility of quartz in H_2O in the lower crust and upper mantle. *Geochimica et Cosmochimica Acta*, *58*(22), 4831–4839. https://doi.org/10.1016/0016-7037(94)90214-3

Marone, C. (1995). Fault zone strength and failure criteria. *Geophysical Research Letters*, *22*(6), 723–726. https://doi.org/10.1029/95gl00268

Marone, C. (1998). The effect of loading rate on static friction and the rate of fault healing during the earthquake cycle. *Nature*, *391*(6662), 69–72. https://doi.org/10.1038/34157

McLaskey, G. C., Thomas, A. M., Glaser, S. D., & Nadeau, R. M. (2012). Fault healing promotes high-frequency earthquakes in laboratory experiments and on natural faults. *Nature*, *491*(7422), 101–104. https://doi.org/10.1038/nature11512

Melosh, B. L., Rowe, C. D., Smit, L., Groenewald, C., Lambert, C. W., & Macey, P. (2014). Snap, Crackle, Pop: Dilational fault breccias record seismic slip below the brittle–plastic transition. *Earth and Planetary Science Letters*, *403*, 432–445. https://doi.org/10.1016/j.epsl.2014.07.002

Menegon, L., Fusseis, F., Stünitz, H., & Xiao, X. (2015). Creep cavitation bands control porosity and fluid flow in lower crustal shear zones. *Geology*, *43*(3), 227–230. https://doi.org/10.1130/g36307.1

Micklethwaite, S. (2009). Mechanisms of faulting and permeability enhancement during epithermal mineralisation: Cracow goldfield, Australia. *Journal of Structural Geology*, *31*(3), 288–300. https://doi.org/10.1016/j.jsg.2008.11.016

Micklethwaite, S., & Cox, S. F. (2004). Fault-segment rupture, aftershock-zone fluid flow, and mineralization. *Geology*, *32*(9), 813–816. https://doi.org/10.1130/G20559.1

Miller, S. A., & Nur, A. (2000). Permeability as a toggle switch in fluid-controlled crustal processes. *Earth and Planetary Science Letters*, *183*(1), 133–146. https://doi.org/10.1016/S0012-821X(00)00263-6

Milliken, K., Reed, R. M., & Laubach, S. E. (2005). Quantifying compaction and cementation in deformation bands in porous sandstones (pp. 237–249). https://doi.org/10.1306/1033726M85252

Mitchell, T. M., Toy, V., Di Toro, G., Renner, J., & Sibson, R. H. (2016). Fault welding by pseudotachylyte formation. *Geology*, *44*(12), 1059–1062. https://doi.org/10.1130/G38373.1

Moncada, D., Mutchler, S., Nieto, A., Reynolds, T., Rimstidt, J., & Bodnar, R. (2012). Mineral textures and fluid inclusion petrography of the epithermal Ag–Au deposits at Guanajuato, Mexico: Application to exploration. *Journal of Geochemical Exploration*, *114*, 20–35. https://doi.org/10.1016/j.gexplo.2011.12.001

Monecke, T., Monecke, J., Reynolds, T. J., Tsuruoka, S., Bennett, M. M., Skewes, W. B., & Palin, R. M. (2018). Quartz solubility in the H_2O-NaCl system: A framework for understanding vein formation in porphyry copper deposits. *Economic Geology*, *113*(5), 1007–1046. https://doi.org/10.5382/econgeo.2018.4580

Mottram, C. M., Kellett, D., Barresi, T., Zwingmann, H., Friend, M., Todd, A., & Percival, J. (2020). Syncing fault rock clocks: Direct comparison of U-Pb carbonate and K-Ar illite fault dating methods. *Geology*, 352267. https://doi.org/10.1130/abs/2020am-352267

Muhuri, S. K., Dewers, T. A., Scott, T. E., Jr., & Reches, Z. (2003). Interseismic fault strengthening and earthquake-slip instability: Friction or cohesion? *Geology*, *31*(10), 881–884. https://doi.org/10.1130/g19601.1

Muir-wood, R., & King, G. (1993). Hydrological signatures of earthquake strain. *Journal of Geophysical Research*, *98*(B12), 22068.

Mullis, A. M. (1991). The role of silica precipitation kinetics in determining the rate of quartz pressure solution. *Journal of Geophysical Research*, *96*(B6), 10007–10013. https://doi.org/10.1029/91jb00683

Nagy, K., & Lasaga, A. (1992). Dissolution and precipitation kinetics of gibbsite at 80°C and pH 3: The dependence on solution saturation state. *Geochimica et Cosmochimica Acta*, *56*(8), 3093–3111. https://doi.org/10.1016/0016-7037(92)90291-p

Nesbitt, B. E., Muehlenbachs, K., & Murowchick, J. B. (1989). Genetic implications of stable isotope characteristics of mesothermal Au deposits and related Sb and Hg deposits in the Canadian Cordillera. *Economic Geology*, *84*(6), 1489–1506. https://doi.org/10.2113/gsecongeo.84.6.1489

Newell, D. L., Jessup, M. J., Hilton, D. R., Shaw, C. A., & Hughes, C. A. (2015). Mantle-derived helium in hot springs of the Cordillera Blanca, Peru: Implications for mantle-to-crust fluid transfer in a flat-slab subduction setting. *Chemical Geology*, *417*, 200–209. https://doi.org/10.1016/j.chemgeo.2015.10.003

Newton, R. C., & Manning, C. E. (2000). Quartz solubility in H_2O-NaCl and H_2O-CO_2 solutions at deep crust-upper mantle pressures and temperatures: 2–15 kbar and 500–900°C. *Geochimica et Cosmochimica Acta*, *64*(17), 2993–3005. https://doi.org/10.1016/s0016-7037(00)00402-6

Nguyen, P. T., Harris, L. B., Powell, C. M., & Cox, S. F. (1998). Fault-valve behaviour in optimally oriented shear zones: An example at the revenge gold mine, Kambalda, Western Australia. *Journal of Structural Geology*, *20*(12), 1625–1640. https://doi.org/10.1016/s0191-8141(98)00054-6

Niemeijer, A., Marone, C., & Elsworth, D. (2008). Healing of simulated fault gouges aided by pressure solution: Results from rock analog experiments. *Journal of Geophysical Research*, *113*(B4). https://doi.org/10.1029/2007JB005376

Nishiyama, N., Sumino, H., & Ujiie, K. (2020). Fluid overpressure in subduction plate boundary caused by mantle-derived fluids. *Earth and Planetary Science Letters*, *538*, 116199. https://doi.org/10.1016/j.epsl.2020.116199

Nuriel, P., Miller, D. M., Schmidt, K. M., Coble, M. A., & Maher, K. (2019). Ten-million years of activity within the Eastern California Shear Zone from U–Pb dating of fault-zone opal. *Earth and Planetary Science Letters*, *521*, 37–45. https://doi.org/10.1016/j.epsl.2019.05.047

O'Hara, K., Mizoguchi, K., Shimamoto, T., & Hower, J. C. (2006). Experimental frictional heating of coal gouge at seismic slip rates: Evidence for devolatilization and thermal pressurization of gouge fluids. *Tectonophysics*, *424*(1–2), 109–118. https://doi.org/10.1016/j.tecto.2006.07.007

Okamoto, A., & Sekine, K. (2011). Textures of syntaxial quartz veins synthesized by hydrothermal experiments. *Journal of Structural Geology*, *33*(12), 1764–1775. https://doi.org/10.1016/j.jsg.2011.10.004

Olsen, M. P., Scholz, C. H., & Léger, A. (1998). Healing and sealing of a simulated fault gouge under hydrothermal conditions: Implications for fault healing. *Journal of Geophysical Research*, *103*(B4), 7421–7430. https://doi.org/10.1029/97jb03402

Onasch, C. M., Farver, J. R., & Dunne, W. M. (2010). The role of dilation and cementation in the formation of cataclasite in low temperature deformation of well cemented quartz-rich rocks. *Journal of Structural Geology*, *32*(12), 1912–1922. https://doi.org/10.1016/j.jsg.2010.04.013

Palandri, J. L., & Kharaka, Y. K. (2004). *A compilation of rate parameters of water-mineral interaction kinetics for application to geochemical modeling* (Tech. Rep.). Geological Survey.

Parry, W., & Bruhn, R. (1990). Fluid pressure transients on seismogenic normal faults. *Tectonophysics*, *179*(3–4), 335–344. https://doi.org/10.1016/0040-1951(90)90299-n

Peacock, D., Dimmen, V., Rotevatn, A., & Sanderson, D. (2017). A broader classification of damage zones. *Journal of Structural Geology*, *102*, 179–192. https://doi.org/10.1016/j.jsg.2017.08.004

Pitcairn, I. K., Craw, D., & Teagle, D. A. (2014). The gold conveyor belt: Large-scale gold mobility in an active orogen. *Ore Geology Reviews*, *62*, 129–142. https://doi.org/10.1016/j.oregeorev.2014.03.006

Pollington, A. D., Kozdon, R., Anovitz, L. M., Georg, R. B., Spicuzza, M. J., & Valley, J. W. (2016). Experimental calibration of silicon and oxygen isotope fractionations between quartz and water at 250°C by in situ microanalysis of experimental products and application to zoned low δ30Si quartz overgrowths. *Chemical Geology*, *421*, 127–142. https://doi.org/10.1016/j.chemgeo.2015.11.011

Ramsay, J. G. (1980). The crack–seal mechanism of rock deformation. *Nature*, *284*(5752), 135–139. https://doi.org/10.1038/284135a0

Rempel, A. W., & Rice, J. R. (2006). Thermal pressurization and onset of melting in fault zones. *Journal of Geophysical Research*, *111*(B9). https://doi.org/10.1029/2006JB004314

Renard, F., Andréani, M., Boullier, A.-M., & Labaume, P. (2005). Crack-seal patterns: Records of uncorrelated stress release variations in crustal rocks. *Geological Society, London, Special Publications*, *243*(1), 67–79. https://doi.org/10.1144/gsl.sp.2005.243.01.07

Renard, F., Gratier, J.-P., & Jamtveit, B. (2000). Kinetics of crack-sealing, intergranular pressure solution, and compaction around active faults. *Journal of Structural Geology*, *22*(10), 1395–1407. https://doi.org/10.1016/s0191-8141(00)00064-x

Rimstidt, J. D., & Barnes, H. L. (1980). The kinetics of silica-water reactions. *Geochimica et Cosmochimica Acta*, *44*(11), 1683–1699. https://doi.org/10.1016/0016-7037(80)90220-3

Rimstidt, J. D., & Cole, D. R. (1983). Geothermal mineralization; I: The mechanism of formation of the Beowawe, Nevada, siliceous sinter deposit. *American Journal of Science*, *283*(8), 861–875. https://doi.org/10.2475/ajs.283.8.861

Robert, F., Boullier, A.-M., & Firdaous, K. (1995). Gold-quartz veins in metamorphic terranes and their bearing on the role of fluids in faulting. *Journal of Geophysical Research*, *100*(B7), 12861–12879. https://doi.org/10.1029/95JB00190

Roberts, N. M., Drost, K., Horstwood, M. S., Condon, D. J., Chew, D., Drake, H., et al. (2020). Laser ablation inductively coupled plasma mass spectrometry (LA-ICP-MS) U-Pb carbonate geochronology: Strategies, progress, and limitations. *Geochronology*, *2*(1), 33–61. https://doi.org/10.5194/gchron-2-33-2020

Rowe, C. D., Lamothe, K., Rempe, M., Andrews, M., Mitchell, T. M., Di Toro, G., et al. (2019). Earthquake lubrication and healing explained by amorphous nanosilica. *Nature Communications*, *10*(1), 1–11. https://doi.org/10.1038/s41467-018-08238-y

Rowe, C. D., Ross, C., Swanson, M. T., Pollock, S., Backeberg, N. R., Barshi, N. A., et al. (2018). Geometric complexity of earthquake rupture surfaces preserved in pseudotachylyte networks. *Journal of Geophysical Research: Solid Earth*, *123*(9), 7998–8015. https://doi.org/10.1029/2018jb016192

Rowland, J. V., & Simmons, S. F. (2012). Hydrologic, magmatic, and tectonic controls on hydrothermal flow, Taupo Volcanic Zone, New Zealand: Implications for the formation of epithermal vein deposits. *Economic Geology*, *107*(3), 427–457. https://doi.org/10.2113/econgeo.107.3.427

Rutter, E. H. (1983). Pressure solution in nature, theory and experiment. *Journal of the Geological Society*, *140*(5), 725–740. https://doi.org/10.1144/gsjgs.140.5.0725

Rutter, E. H., & Elliott, D. (1976). The kinetics of rock deformation by pressure solution (and discussion). *Philosophical Transactions of the Royal Society of London – A*, *283*, 203–219. https://doi.org/10.1098/rsta.1976.0079

Saishu, H., Okamoto, A., & Otsubo, M. (2017). Silica precipitation potentially controls earthquake recurrence in seismogenic zones. *Scientific Reports*, *7*(1), 1–10. https://doi.org/10.1038/s41598-017-13597-5

Saishu, H., Okamoto, A., & Tsuchiya, N. (2014). The significance of silica precipitation on the formation of the permeable–impermeable boundary within Earth's crust. *Terra Nova*, *26*(4), 253–259. https://doi.org/10.1111/ter.12093

Sanchez-Alfaro, P., Reich, M., Driesner, T., Cembrano, J., Arancibia, G., Pérez-Flores, P., et al. (2016). The optimal windows for seismically-enhanced gold precipitation in the epithermal environment. *Ore Geology Reviews*, *79*, 463–473. https://doi.org/10.1016/j.oregeorev.2016.06.005

Scheiber, T., Viola, G., van der Lelij, R., Margreth, A., & Schönenberger, J. (2019). Microstructurally-constrained versus bulk fault gouge K-Ar dating. *Journal of Structural Geology*, *127*, 103868. https://doi.org/10.1016/j.jsg.2019.103868

Sibson, R., & Scott, J. (1998). Stress/fault controls on the containment and release of overpressured fluids: Examples from gold-quartz vein systems in Juneau, Alaska; Victoria, Australia and Otago, New Zealand. *Ore Geology Reviews*, *13*(1), 293–306. https://doi.org/10.1016/S0169-1368(97)00023-1

Sibson, R. H. (1982). Fault zone models, heat flow, and the depth distribution of earthquakes in the continental crust of the United States. *Bulletin of the Seismological Society of America*, *72*(1), 151–163.

Sibson, R. H. (1986). Brecciation processes in fault zones: Inferences from earthquake rupturing. *Pure and Applied Geophysics PAGEOPH*, *124*(1–2), 159–175. https://doi.org/10.1007/BF00875724

Sibson, R. H. (1987). Earthquake rupturing as a mineralizing agent in hydrothermal systems. *Geology*, *15*(8), 701–704. https://doi.org/10.1130/0091-7613(1987)15<701:eraama>2.0.co;2

Sibson, R. H. (1989). Earthquake faulting as a structural process. *Journal of Structural Geology*, *11*(1/2), 1–14. https://doi.org/10.1016/0191-8141(89)90032-1

Sibson, R. H. (1990). Conditions for fault-valve behaviour. *Geological Society, London, Special Publications*, *54*(1), 15–28. https://doi.org/10.1144/gsl.sp.1990.054.01.02

Sibson, R. H. (1992). Implications of fault-valve behaviour for rupture nucleation and recurrence. *Tectonophysics*, *211*(1–4), 283–293. https://doi.org/10.1016/0040-1951(92)90065-e

Sibson, R. H. (1994). Crustal stress, faulting and fluid flow. *Geological Society, London, Special Publications*, *78*(1), 69–84. https://doi.org/10.1144/GSL.SP.1994.078.01.07

Sibson, R. H. (1995). Selective fault reactivation during basin inversion: Potential for fluid redistribution through fault-valve action. *Geological Society, London, Special Publications*, *88*(1), 3–19. https://doi.org/10.1144/gsl.sp.1995.088.01.02

Sibson, R. H. (1996). Structural permeability of fluid-driven fault-fracture meshes. *Journal of Structural Geology*, *18*(8), 1031–1042. https://doi.org/10.1016/0191-8141(96)00032-6

Sibson, R. H. (2003). Brittle-failure controls on maximum sustainable overpressure in different tectonic regimes. *AAPG Bulletin*, *87*(6), 901–908. https://doi.org/10.1306/01290300181

Sibson, R. H. (2017). Tensile overpressure compartments on low-angle thrust faults. *Earth Planets and Space*, *69*(1), 113. https://doi.org/10.1186/s40623-017-0699-y

Sibson, R. H., Moore, J. M. M., & Rankin, A. H. (1975). Seismic pumping—A hydrothermal fluid transport mechanism. *Journal of the Geological Society*, *131*(6), 653–659. https://doi.org/10.1144/gsjgs.131.6.0653

Sibson, R. H., Robert, F., & Poulsen, K. H. (1988). High-angle reverse faults, fluid-pressure cycling, and mesothermal gold-quartz deposits. *Geology*, *16*(6), 551–555. https://doi.org/10.1130/0091-7613(1988)016<0551:harffp>2.3.co;2

Sibson, R. H., & Rowland, J. V. (2003). Stress, fluid pressure and structural permeability in seismogenic crust, North Island, New Zealand. *Geophysical Journal International*, *154*(2), 584–594. https://doi.org/10.1046/j.1365-246x.2003.01965.x

Smeraglia, L., Berra, F., Billi, A., Boschi, C., Carminati, E., & Doglioni, C. (2016). Origin and role of fluids involved in the seismic cycle of extensional faults in carbonate rocks. *Earth and Planetary Science Letters*, *450*, 292–305. https://doi.org/10.1016/j.epsl.2016.06.042

Spruženiece, L., Späth, M., Urai, J. L., Ukar, E., Selzer, M., & Nestler, B. (2021). Wide-blocky veins explained by dependency of crystal growth rate on fracture surface type: Insights from phase-field modeling. *Geology*, *49*(6), 641–646. https://doi.org/10.1130/G48472.1

Stenvall, C. A., Fagereng, A., Diener, J. F. A., Harris, C., & Janney, P. E. (2020). Sources and effects of fluids in continental retrograde shear zones: Insights from the Kuckaus Mylonite Zone, Namibia. *Geofluids*, *2020*, 3023268. https://doi.org/10.1155/2020/3023268

Taetz, S., John, T., Bröcker, M., Spandler, C., & Stracke, A. (2018). Fast intraslab fluid-flow events linked to pulses of high pore fluid pressure at the subducted plate interface. *Earth and Planetary Science Letters*, *482*, 33–43. https://doi.org/10.1016/j.epsl.2017.10.044

Tenthorey, E., & Cox, S. F. (2006). Cohesive strengthening of fault zones during the interseismic period: An experimental study. *Journal of Geophysical Research*, *111*(B9), B09202. https://doi.org/10.1029/2005jb004122

Tenthorey, E., Cox, S. F., & Todd, H. F. (2003). Evolution of strength recovery and permeability during fluid–rock reaction in experimental fault zones. *Earth and Planetary Science Letters*, *206*(1–2), 161–172. https://doi.org/10.1016/s0012-821x(02)01082-8

Ujiie, K., Saishu, H., Fagereng, Å., Nishiyama, N., Otsubo, M., Masuyama, H., & Kagi, H. (2018). An explanation of episodic tremor and slow slip constrained by crack-seal veins and viscous shear in subduction mélange. *Geophysical Research Letters*, *45*(11), 5371–5379. https://doi.org/10.1029/2018gl078374

Uysal, I. T., Feng, Y.-x., Zhao, J.-x., Bolhar, R., Işik, V., Baublys, K. A., et al. (2011). Seismic cycles recorded in late quaternary calcite veins: Geochronological, geochemical and microstructural evidence. *Earth and Planetary Science Letters*, *303*(1–2), 84–96. https://doi.org/10.1016/j.epsl.2010.12.039

van den Ende, M., & Niemeijer, A. (2018). Time-dependent compaction as a mechanism for regular stick-slips. *Geophysical Research Letters*, *45*(12), 5959–5967. https://doi.org/10.1029/2018gl078103

Van den Ende, M., & Niemeijer, A. (2019). An investigation into the role of time-dependent cohesion in interseismic fault restrengthening. *Scientific Reports*, *9*(1), 1–11. https://doi.org/10.1038/s41598-019-46241-5

Vrolijk, P. (1987a). Tectonically driven fluid flow in the Kodiak accretionary complex, Alaska. *Geology*, *15*(5), 466–469. https://doi.org/10.1130/0091-7613(1987)15<466:tdffit>2.0.co;2

Vrolijk, P. (1987b). Paleohydrogeology and fluid evolution of the Kodiak accretionary complex, Alaska (Ph.D. thesis). University of California.

Wagner, W., & Kretzschmar, H.-J. (2008). IAPWS industrial formulation 1997 for the thermodynamic properties of water and steam. *International Steam Tables: Properties of Water and Steam Based on the Industrial Formulation IAPWS-IF97* (pp. 7–150).

Wang, Q., Laubach, S., & Fall, A. (2019). Coupled effects of diagenesis and deformation on fracture evolution in deeply buried sandstones. In *53rd US Rock Mechanics/Geomechanics Symposium*. OnePetro.

Wang, Y., Bryan, C., Xu, H., & Gao, H. (2003). Nanogeochemistry: Geochemical reactions and mass transfers in nanopores. *Geology*, *31*(5), 387–390. https://doi.org/10.1130/0091-7613(2003)031<0387:ngramt>2.0.co;2

Watson, E. B., & Wark, D. A. (1997). Diffusion of dissolved SiO_2 in H_2O at 1 GPa, with implications for mass transport in the crust and upper mantle. *Contributions to Mineralogy and Petrology*, *130*(1), 66–80. https://doi.org/10.1007/s004100050350

Weatherley, D. K., & Henley, R. W. (2013). Flash vaporization during earthquakes evidenced by gold deposits. *Nature Geoscience*, *6*(4), 294–298. https://doi.org/10.1038/ngeo1759

Weir, R. H., & Kerrick, D. (1987). Mineralogic, fluid inclusion, and stable isotope studies of several gold mines in the Mother Lode, Tuolumne and Mariposa counties, California. *Economic Geology*, *82*(2), 328–344. https://doi.org/10.2113/gsecongeo.82.2.328

Wibberley, C. A., & Shimamoto, T. (2005). Earthquake slip weakening and asperities explained by thermal pressurization. *Nature*, *436*(7051), 689–692. https://doi.org/10.1038/nature03901

Williams, R., Goodwin, L., & Mozley, P. (2016). Diagenetic controls on the evolution of fault-zone architecture and permeability structure: Implications for episodicity of fault-zone fluid transport in extensional basins. *Bulletin of the Geological Society of America*, *129*(3–4), 464–478. https://doi.org/10.1130/B31443.1

Williams, R. T. (2019). Coseismic boiling cannot seal faults: Implications for the seismic cycle. *Geology*, *47*(5), 461–464. https://doi.org/10.1130/g45936.1

Williams, R. T., Beard, B. L., Goodwin, L. B., Sharp, W. D., Johnson, C. M., & Mozley, P. S. (2019). Radiogenic isotopes record a 'drop in a bucket' – A fingerprint of multi-kilometer-scale fluid pathways inferred to drive fault-valve behavior. *Journal of Structural Geology*, *125*, 262–269. https://doi.org/10.1016/j.jsg.2018.07.023

Williams, R. T., Davis, J. R., & Goodwin, L. B. (2019). Do large earthquakes occur at regular intervals through time? A perspective from the geologic record. *Geophysical Research Letters*, *46*(14), 8074–8081. https://doi.org/10.1029/2019gl083291

Williams, R. T., Farver, J. R., Onasch, C. M., & Winslow, D. F. (2015). An experimental investigation of the role of microfracture surfaces in controlling quartz precipitation rate: Applications to fault zone diagenesis. *Journal of Structural Geology*, *74*, 24–30. https://doi.org/10.1016/j.jsg.2015.02.011

Williams, R. T., Goodwin, L. B., Mozley, P. S., Beard, B. L., & Johnson, C. M. (2015). Tectonic controls on fault zone flow pathways in the Rio Grande rift, New Mexico, USA. *Geology*, *43*(8), 723–726. https://doi.org/10.1130/G36799.1

Williams, R. T., Mozley, P. S., Sharp, W. D., & Goodwin, L. B. (2019). U-Th dating of syntectonic calcite veins reveals the dynamic nature of fracture cementation and healing in faults. *Geophysical Research Letters*, *46*(2212), 900908–900912. https://doi.org/10.1029/2019gl085403

Woodcock, N., Dickson, J., & Tarasewicz, J. (2007). Transient permeability and reseal hardening in fault zones: Evidence from dilation breccia textures. *Geological Society, London, Special Publications*, *270*(1), 43–53. https://doi.org/10.1144/gsl.sp.2007.270.01.03

Yasuhara, H., Marone, C., & Elsworth, D. (2005). Fault zone restrengthening and frictional healing: The role of pressure solution. *Journal of Geophysical Research*, *110*(B6), B06310. https://doi.org/10.1029/2004JB003327

Yilmaz, T. I., Duschl, F., & Di Genova, D. (2016). Feathery and network-like filamentous textures as indicators for the re-crystallization of quartz from a metastable silica precursor at the Rusey Fault Zone, Cornwall, UK. *Solid Earth*, *7*(6), 1509–1536. https://doi.org/10.5194/se-7-1509-2016

Zhang, S., Cox, S. F., & Paterson, M. S. (1994). The influence of room temperature deformation on porosity and permeability in calcite aggregates. *Journal of Geophysical Research*, *99*(B8), 15761–15775. https://doi.org/10.1029/94jb00647